https://doi.org/10.5194/egusphere-2026-1902
Preprint. Discussion started: 14 April 2026

Modeling the potential hazard of wildfires under the influence of climatic, vegetative and anthropogenic factors in the Andean and Amazonian regions of Peru.

Yerson Ccanchi [1,2] Ricardo Zubieta [1], Josep Prado [3], Jose Sinticala [1]

[1] Dirección de Ciencias de la Atmósfera, Hidrósfera y Cambio Climático, Instituto Geofísico del Perú (IGP), Lima, Perú
[2] Programa de Maestria en Recursos Hídricos, Universidad Nacional Agraria La Molina (UNALM), Lima, Perú.
[3] Subdirección de Estudios e investigaciones Agrometerológicas, Servicio Nacional de Meteorología e Hidrología (SENAMHI), Perú

Correspondence to: R. Zubieta (rzubieta@igp.gob.pe).

Abstract. Wildfires and their associated impacts have increased significantly over the past two decades, heightening the risk to human life and causing substantial damage to forest ecosystems in the Amazon and Andean regions. To mitigate these impacts, the assessment of both seasonal and intra-seasonal wildfire hazard is of critical importance. The availability of satellite data, together with the implementation of regional wildfire early warning systems based on hazard indices, represents a key component in reducing wildfire risk. This study aims to develop a new short-term wildfire hazard model based on both observational and satellite-derived datasets, including data from the Moderate Resolution Imaging Spectroradiometer (MODIS) and the Global Precipitation Measurement (GPM). The proposed Wildfire Hazard Index (WHI) is derived from Dry-Day Frequency (DDF), the Normalized Difference Vegetation Index (NDVI), cultivated area (CA), and forest fuel (FF). A wildfire hazard classification scheme (extreme, very high, high, moderate, and low) is introduced to generate hazard maps. The results indicate that DDF, NDVI, CA, and FF are key variables for analyzing the spatial and temporal variability of wildfire hazard. Lower WHI values correspond to lower wildfire hazard, and vice versa. The findings suggest that the model adequately represents seasonal wildfire hazard, demonstrating consistency among WHI values, wildfire occurrence, and MODIS-derived hotspots. Overall, this study shows that the proposed method can support hazard classification and contribute to the implementation of regional wildfire early warning systems based on precipitation forecasts in the Amazon and Andean regions.

Keywords: Wildfire, Index, Andes, Hazard, Peru, Amazon.

1 INTRODUCTION

In recent decades, wildfire regimes have undergone significant changes worldwide (Keeley and Syphard, 2021; Li et al., 2026; Schmidt and Eloy, 2020). On average, between 1995 and 2015, approximately 1.46 million hectares of tropical rainforest were lost annually (Hirschberger, 2016). In 2019, the highest wildfire occurrence in tropical regions of South America over the past 20 years was recorded (Silva et al., 2021). Wildfires and deforestation represent the principal threats to the Amazon in tropical regions (dos Reis et al., 2021). For instance, 10,897 km² of forest were cleared, and cumulative forest loss in the Brazilian Amazon reached 820,000 km² by 2020 (INPE, 2021). Wildfires in forested areas of South America can be regarded as environmental disasters, often triggered by anthropogenic activities (Alvarez et al., 2025; Pivello et al., 2021; Taboada-Hermoza and Martínez, 2025). A wildfire is defined as an unplanned and uncontrolled fire that occurs in natural areas, often unexpectedly, and may develop into a destructive event, causing damage to natural

https://doi.org/10.5194/egusphere-2026-1902
Preprint. Discussion started: 14 April 2026

resources and ecosystems while posing a threat to human life. Wildfire hazard has been extensively studied since 1925, incorporating various static and dynamic factors, both cumulative and non-cumulative (Bradshaw et al., 1984; Burgan, 1988; Van Wagner, 1987). These studies have led to the development of numerous wildfire indices at different spatial scales (Chen et al., 2023; Laneve et al., 2020; Soto et al., 2015; Xofis et al., 2020). However, the reliability of these hazard indices varies considerably in space and time, and only a subset has been shown to be effective through validation against actual wildfire occurrences.

Wildfire hazard is influenced by the moisture content of combustible materials, meteorological conditions, and topography (Rothermel, 1972; Van Wagner, 1987). Climate variability has contributed to an increase in the frequency of extreme climatic events in Andean and Amazonian ecosystems of South America, highlighting their vulnerability to climate change (Acevedo Ortiz et al., 2026; dos Reis et al., 2021; Zubieta et al., 2019), particularly in terms of impacts on flora and fauna due to wildfires (Mosquera-Guerra et al., 2024). A primary driver is the use of fire in agricultural and livestock practices, where burns often spread uncontrollably, leading to severe impacts (Alvarez et al., 2025; Taboada-Hermoza and Martínez, 2025). Monitoring of fire activity and wildfire hazard is therefore essential for preventive management and constitutes a critical component of early warning systems (Zubieta et al., 2023a; Mestre and Manta, 2014).

The Andean and Amazonian regions of South America exhibit exceptionally high forest diversity (Fearnside, 2017). Alterations to these ecosystems underscore the urgent need to preserve their integrity at large spatial scales to maintain local tree diversity (Fadrique et al., 2026). However, the increasing frequency of wildfires over the past two decades poses a significant threat to the conservation of tree species in both the Andes and the Amazon (Pivello et al., 2021; Zubieta et al., 2021a). This increase has been linked to factors such as droughts and extreme wind events in these regions (Ccanchi, 2021; Toledo et al., 2024; Zubieta et al., 2023b), which contribute to moisture loss and heightened exposure of vegetative fuels. Notable examples include severe droughts in 2005 (Marengo et al., 2008), 2010 (Espinoza et al., 2012; Marengo and Espinoza, 2016), 2016 (Jimenez et al., 2021), and the 2019–2022 dry period associated with El Niño (Geirinhas et al., 2023) in the Andean and Amazonian regions. Tropical regions of South America have consistently experienced severe wildfire crises due to burning activities coinciding with prolonged drought conditions linked to climate variability (Acevedo Ortiz et al., 2026; Pivello et al., 2021; Sulca et al., 2021; Zubieta et al., 2021b, 2023b). To prevent burns from escalating into wildfires, continuous monitoring of climatic conditions that influence wildfire spread is a crucial measure (Carta et al., 2023).

To characterize wildfire hazard, an initial approximation has been developed using the Fire Weather Index at large spatial scales (Chandler et al., 1983; Van Wagner, 1987). Ensuring the safety of local populations and firefighters requires continuous monitoring of the spatial and temporal distribution of vegetation conditions and the effects of drought (Artés et al., 2022). In this context, technical parameters derived from dry conditions are particularly useful for characterizing wildfire hazard. These include cumulative drought conditions (Zubieta et al., 2021b), forest fuel load (Fernandes, 2009), fuel treatment effectiveness (Hood et al., 2022), topographic factors such as elevation (Bountzouklis et al., 2023; Qadir et al., 2021), and temporal and spatial patterns of fire occurrence (Schmidt and Eloy, 2020).

Applications of wildfire hazard indices in South America have been reported in Brazil (Alcarde Alvares et al., 2014; Nunes et al., 2006; Silva et al., 2020), Argentina (Marcuzzi et al., 2022; Waidelich et al., 2019), Ecuador (Pazmiño, 2019), and Colombia (Camargo Caicedo et al., 2025). Additionally, advances in wildfire hazard assessment using artificial intelligence have been proposed for the Chilean region in southwestern South America (Gajardo et al., 2025). However, their applicability to the Andean–Amazonian regions of Peru has not yet been rigorously evaluated in the scientific literature. This study aims to propose a simplified model to assess wildfire hazard potential under the influence of climatic and vegetation-related factors in the Andean and Amazonian regions of Peru.

https://doi.org/10.5194/egusphere-2026-1902
Preprint. Discussion started: 14 April 2026

2 Study area.

The Andes Mountains and the Amazon region of Peru extend along the western margin of South America (Fig. 1). Peru comprises distinct geographical zones, including arid coastal regions in the west, three mountain systems of the Andean Cordillera (Western, Eastern, and Sub-Andean Cordilleras) across the central belt (Fig. 1), and predominantly tropical forests extending over the eastern part of the country (Pulgar Vidal, 2014). Figure 1 illustrates an approximation of Peru's three principal geographical regions—coastal (1, 2, and 3), Andean (4, 5, and 6), and Amazonian (7, 8, and 9)—used in this study to analyze wildfire hazard (Cubas, 2021). The Andes represent one of the most important biodiversity hotspots in the world (Bax and Francesconi, 2019; Myers et al., 2000), and the Amazonian and Andean ecosystems of Peru are recognized as conservation priorities because of their exceptional biodiversity, including a high diversity of plant and vertebrate species (Asner et al., 2017).

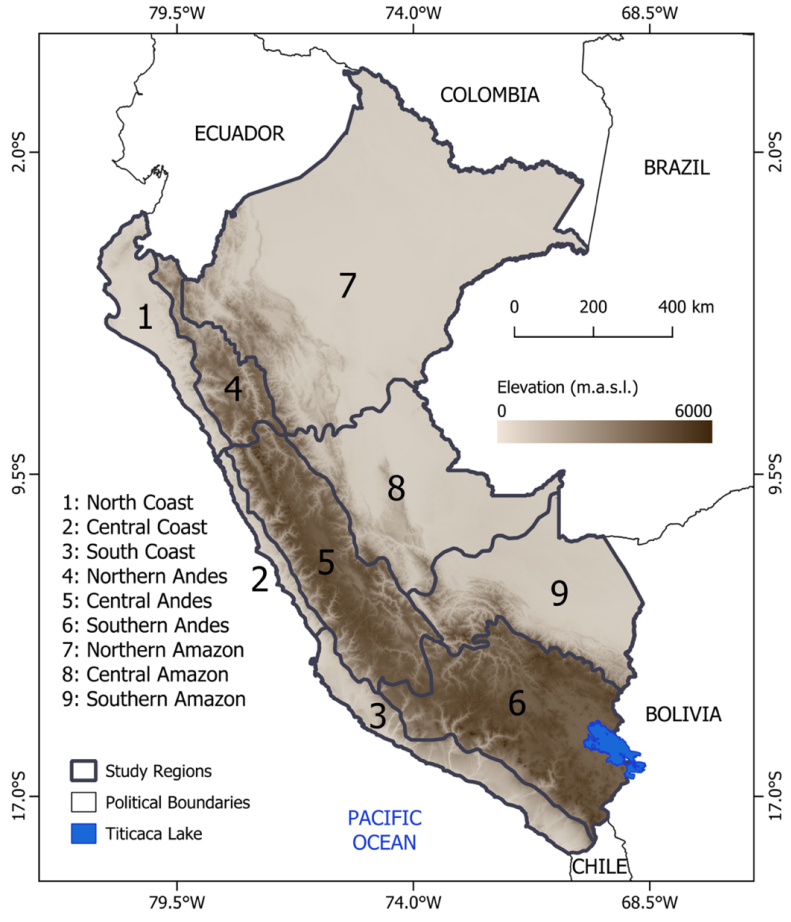

Figure 1: Study area and areas of analysis proposed.

https://doi.org/10.5194/egusphere-2026-1902
Preprint. Discussion started: 14 April 2026

Annual precipitation patterns vary markedly across the country. The highest precipitation (exceeding 1000 mm/year) occurs predominantly in the tropical forests of eastern Peru, whereas the Andean region experiences lower values, ranging from 350 to 1300 mm/year (Espinoza Villar et al., 2009). Under climate change scenarios, an increase in extreme precipitation events is expected to coincide with more frequent and intense meteorological droughts, characterized by reduced precipitation and increased evapotranspiration in the Peruvian Andes (Potter et al., 2023; Zubieta et al., 2021a). Extreme drought events, such as those recorded in 2005, 2010, 2016, 2020, and 2022, have been strongly associated with more frequent wildfire occurrence in Peru, with increases ranging from 400% to 700% compared to historical averages (Zubieta et al., 2019, 2023b).

For comparative purposes, this study defines the Andean region as reference areas located above 1500 meters above sea level (masl) (Zubieta et al., 2021b), while the Amazon region is considered to comprise lowlands up to 1500 masl on the eastern slopes of the Andes (Fig. 1). Official wildfire records from the Peruvian government, supported by data from the Civil Defense Institute, indicate that 80–90% of wildfire occurrences are concentrated in the Andean region, particularly between 1500 and 4000 masl (Zubieta et al., 2021b). Andean grasslands constitute the ecosystem at greatest risk of wildfire in high-altitude regions (Ccanchi, 2021; Zubieta et al., 2021b), where the accumulation of highly flammable vegetation could significantly increase wildfire hazard, especially during the dry season (June–August) and the onset of the wet season (September–December). The agricultural sector, in which the use of fire is common, employs the largest proportion of the Peruvian workforce (27.5%) (UP, 2022). Despite its economic importance, however, the hazards associated with fire use in agriculture and livestock production have received relatively limited scientific attention (Alvarez et al., 2025; Taboada-Hermoza and Martínez, 2025). A recent study highlights that wildfires—officially recognized as emergencies by governmental authorities—in the Andean region of Cusco (southern Peru) are primarily located near rivers and roads (Zubieta et al., 2023a).

The availability of climate datasets in Peru, including observational data (Aybar et al., 2020), satellite-based precipitation products (Huffman et al., 2023), and vegetation spectral indices derived from satellite observations (Ccanchi, 2021; Zubieta et al., 2021b), provides a valuable opportunity to analyze wildfire hazard and develop new prevention methodologies (Ambadan et al., 2020; Laneve et al., 2020; Talukdar et al., 2024). Given Peru's extensive biodiversity and diverse natural regions, the implementation of such methodologies should consider the specific environmental conditions of the Pacific slope, the eastern Andean region, and the Amazon basin

3 Data and Methodology

3.1 Datasets

Historical data on wildfire locations were compiled from the Ministry of the Environment of Peru (MINAM, 2025), constructed form emergency reports prepared by the National Institute of Civil Defense. MODIS surface reflectance data (MOD09A1 product) were obtained at a spatial resolution of 500 m and a temporal resolution of 8 days. To minimize atmospheric interference and ensure the reliability of the spectral signal, the MODIS quality band (StateQA) was applied, providing a robust basis for deriving vegetation parameters (Vermote et al., 2002). Daily precipitation data were obtained from the GPM-IMERG Late Run product at a spatial resolution of 0.1° (~10 km) (Huffman et al., 2023). Additionally, thermal anomalies (hotspots) were retrieved from the NASA FIRMS (MODIS MCD14DL product) at 1 km resolution (Giglio et al., 2018).

https://doi.org/10.5194/egusphere-2026-1902
Preprint. Discussion started: 14 April 2026

To differentiate between vegetation cover and agricultural areas, the National Vegetation Cover Map (MINAM, 2019) and the National Agricultural Area Map (MIDAGRI, 2024) were used, respectively. Areas under cultivation, where the use of fire is common, were characterized using data from the National Survey of Planting Intentions (NSPI) for the period 2020–2025 (MIDAGRI, 2025a). This survey provides monthly statistics on temporary crops (hectares planned for cultivation) at the district level. Finally, for comparison, monthly wildfire hazard maps for Peru, developed by MINAM (2025) based on the Index of Favorable Conditions for Fires in Vegetation (CFOI), were also collected for the period 2021–2025.

3.2 Methodology

To account for Peru's diverse climatic regions (Cubas, 2021), the study was structured using a regional sectorization adapted from the SENAMHI climate classification, dividing the country into nine homogeneous regions across the Coast, Highlands, and Rainforest (Fig. 1). To standardize spatial resolution, climatic, satellite, and cartographic variables were integrated into a 0.1° (~10 km) grid, allowing interoperability among datasets from different sources.

To analyze fire activity from MODIS and reduce the uncertainty of this satellite product (Ccanchi and Zubieta 2024), thermal anomalies (hotspots) were preprocessed to remove false positives associated with glaciers, volcanoes, and identified urban areas. Anthropogenic, climatic, and vegetation-related factors influencing wildfire hazard were then selected as input variables for the hazard model. A schematic representation of the modeling framework is presented in Figure 2.

3.2.1 Input variables to wildfire hazard modeling

To analyze the dynamic nature of wildfire hazard, indicators capturing the temporal and seasonal variability of drought conditions and vegetation status were employed. These factors, derived from remote sensing data, enable continuous updating of hazard levels based on moisture conditions and vegetation response (Ccanchi, 2021; Zubieta et al., 2021b, 2023b). The dry season plays a cumulative role in reducing vegetation moisture (Zubieta et al., 2021b). This water stress indicator is assessed through the accumulation of Dry-Day Frequency (DDF) over the previous 30 days (Espinoza et al., 2016; Saavedra and Zubieta, 2024). For this purpose, precipitation data from the GPM-IMERG Late Run product were used (Huffman et al., 2023). A "dry day" is operationally defined as a day with accumulated precipitation below 1 mm (Espinoza et al., 2016), a criterion also applied in studies conducted in the Peruvian Andes (Zubieta et al., 2021b; Ccanchi, 2021).

To standardize the response of this parameter within the model, the DDF was normalized using the historical 75th (P_{75}) and 99th (P_{99}) percentiles of the 2002–2024 time series. P_{75} was used as the threshold for the onset of significant drought conditions, separating standard climate variability from periods where dry day accumulation exceeds normal levels. This percentile-based criterion follows the statistical rationale used in extreme climate analysis, where the 75th percentile is applied to isolate significant departures from normal atmospheric conditions (Lenderink and van Meijgaard, 2010), while P_{99} was used as the upper bound for extreme drought conditions, following statistical criteria widely applied to identify high-intensity, low-probability climate events (Galeano et al., 2017).

This approach enables the definition of a hazard scaling (last 30 days) function ranging from 0 to 3 for each pixel derived from GPM-IMERG data, as described below:

https://doi.org/10.5194/egusphere-2026-1902
Preprint. Discussion started: 14 April 2026

$$P_{drought} = \begin{cases} 0 & \text{if } DDF_{t,i} \leq P_{75} \\ 3 \times \frac{DDF_{t,i} - P_{75}}{P_{99} - P_{75}} & \text{if } P_{75} < DDF_{t,i} < P_{99} \\ 3 & \text{if } DDF_{t,i} \geq P_{99} \end{cases} \quad t = 1:46\,;\ i = 1:30 \qquad (1)$$

Where $P_{drought}$ represents the climatic parameter in the model, DDF denotes the cumulative number of dry days at time *t*, calculated for each day *i* over the preceding 30-day period. "*t*" refers to the annual MODIS availability; "*i*" refers to the last 30 days.

The effects of drought conditions, or reduced precipitation, on vegetation were assessed based on vegetation dynamics. Vegetation status was characterized using the Normalized Difference Vegetation Index (NDVI) (Rouse et al., 1974), derived from the MOD09A1 MODIS product. This vegetation-related component enables the identification of water stress and reductions in biomass vigor, which are key factors influencing the flammability of live fuels during periods without rainfall (Zubieta et al., 2021b).

To ensure comparability within the model, NDVI was normalized on a scale from 0 to 3 using the historical time series for the period 2002–2024. The normalization procedure compares current vegetation vigor with the historical maximum average value ($NDVI_{max}$) observed in April (the period of peak vegetative vigor) and a critical wilting threshold, defined as the 1st percentile (P_1) of the historical NDVI distribution. P_1 was selected to represent the lower bound of historically observed extreme low vegetation conditions, where only 1% of the historical record falls below this level, consistent with the use of low-order percentiles to characterize extreme states in vegetation time series (Forkel et al., 2013) as described below:

$$Veg_{dry} = \begin{cases} 0 & \text{if } NDVI_t \geq NDVI_{max} \\ 3 \times \frac{NDVI_{max} - NDVI_t}{NDVI_{max} - P_1} & \text{if } P_1 < NDVI_t < NDVI_{max} \\ 3 & \text{if } NDVI_t \leq P_1 \end{cases} \quad t = 1:46 \qquad (2)$$

Where Veg_{dry} represents the vegetation-related parameter of the model, and NDVI (average of the last 4 images), *t* denotes the spectral index at time *t.*

To account for the role of human activity associated with fire use in the agricultural and livestock sectors (ignition agent) ($Agr_{fire\ use}$), this component was incorporated as a monthly dynamic variable. This variable is directly linked to the planting calendar, which typically involves the use of fire for land clearing and preparation prior to sowing (Alvarez et al., 2025). For its estimation, the planned area of temporary crops for the 2020–2025 seasons at the district level was used (MIDAGRI, 2025b). The planting data series was normalized to a scale from 0 to 3 using the 33.3% and 66.6% terciles of the historical distribution for each district. To restrict the analysis to agricultural areas, a vegetation cover map (MIDAGRI, 2024) was overlaid, resulting in twelve maps that characterize fire hazard zones associated with agricultural activity (fire use). Finally, to represent the fuel component (M_{fuel}), defined as the combustible vegetation material, the spatial distribution of vegetation cover was derived from the National Vegetation Cover Map (CENEPRED, 2020) (Fig. 2). Vegetation classes (MINAM, 2019) were reclassified into four hazard levels according to their flammability (CENEPRED, 2020): level 0 for non-combustible areas (e.g., deserts, water bodies, and urban areas), level 1 for tree cover, level 2 for shrub cover, and level 3 for grasslands and pastures.

https://doi.org/10.5194/egusphere-2026-1902
Preprint. Discussion started: 14 April 2026

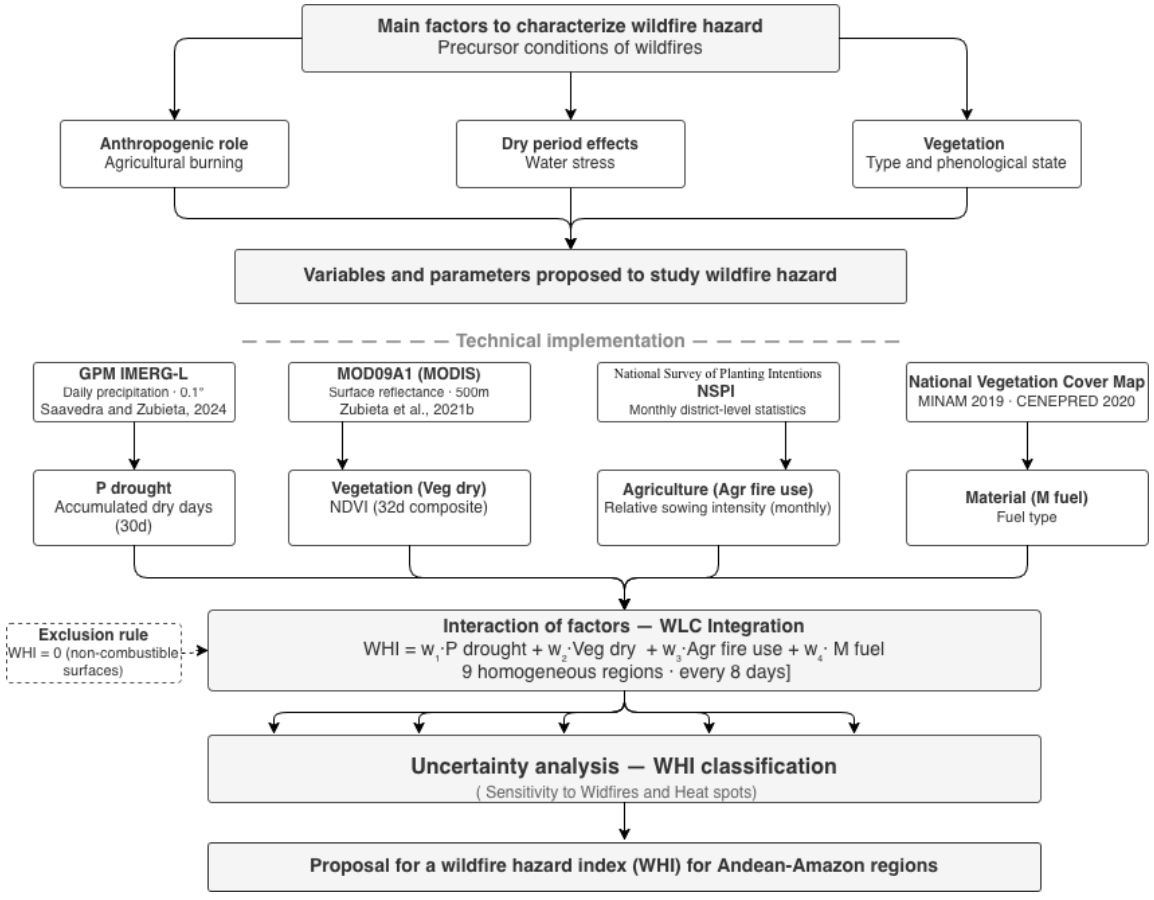

Figure 2: Simplified flowchart of the proposed Wildfire Hazard Index algorithm.

3.2.2 Wildfire Hazard Index (WHI)

Integration of climatic factors ($P_{drought}$), vegetation condition (Veg_{dry}) anthropogenic influences ($Agr_{fire\ use}$), and fuel load (M_{fuel}) was performed using a Weighted Linear Combination (WLC) approach (Fig. 2). Unlike data-driven models that require extensive training datasets, this knowledge-driven approach ensures physical interpretability and remains robust in regions with limited historical records. The relative importance of each factor was determined through a meta-analysis that primarily considered (a) findings from previous wildfire research (Alvarez et al., 2025; Ccanchi, 2021; Espinoza et al., 2016; Zubieta et al., 2021b, 2023b), and (b) the authors' expertise regarding Peru's environmental conditions and biodiversity.

For the assignment of weights in the WLC framework, a pairwise comparison approach based on the Analytic Hierarchy Process (AHP) was applied (Saaty, 1977). This method is widely recognized for multi-criteria evaluation (MCE) in Geographic Information System (GIS) environments, as it enables the integration of variables with different characteristics through the hierarchical assignment of

https://doi.org/10.5194/egusphere-2026-1902
Preprint. Discussion started: 14 April 2026

relative importance. The AHP approach has been successfully applied in various wildfire-related studies (Adaktylou et al., 2020; Eugenio et al., 2016). The general mathematical formulation of the model is defined as follows:

$$WHI = (w_a \cdot P_{Drought}) + (w_b \cdot Veg_{Dry}) + (w_c \cdot Agr_{fire\ use}) + (w_d \cdot M_{fuel}) \quad (3)$$

Where the coefficients w_n represent the relative weights assigned to each factor. To account for the geographic heterogeneity across the nine regions, a sensitivity analysis was performed using differential weighting scenarios grouped into five categories according to the dominant factor: (1) balanced weights, (2) climate dominance, (3) phenological dominance, (4) anthropogenic dominance, and (5) fuel dominance. Within each group, the weight of the dominant factor varied progressively between 0.40 and 0.70, while the remaining weights were distributed complementarily ensuring that their sum equaled 1. The model was implemented at an 8-day temporal resolution, consistent with the MODIS data, while non-combustible surfaces (e.g., sparse vegetation, water bodies, deserts, and urban areas) were excluded from the WHI modeling (Fig. 2). The resulting WHI values range continuously from 0 to 3 and are classified into six hazard levels to facilitate operational interpretation (Table 1).

Table 1: Classification of Wildfire Hazard index (WHI).

WHI Interval	Hazard Class	Level	Description
0	Very low	0	**Sparse or no vegetation.**
>0 & <=0.6	Low	1	**Predominantly humid forest ecosystems**, characterized by absence of agricultural activity and a very limited number of days.
>0.6 & <=1.2	Moderate	2	**Shrubland and/or forest ecosystems of moderate humid** with a probable presence of agricultural activity, where accumulated number of dry days has not exceeded typ levels.
>1.2 & <=1.8	High	3	**Herbaceous, shrubland, and/or forest ecosystems**, wit very high likelihood of agricultural activity, where accumulated number of dry days has led to a reductior vegetation moisture.
>1.8 & <=2.4	Very High	4	**Predominantly herbaceous ecosystems (in addition shrubland and/or forest ecosystems)**, with a very h likelihood of agricultural activity, where the accumula number of dry days exceeds typical levels, resulting in lim vegetation moisture.
>2.4 & <=3	Extreme	5	**Predominantly herbaceous ecosystems, as well as shrubl and/or forest ecosystems**, with a very high likelihood agricultural activity, where the accumulated number of dry d is far above typical levels, leading to a severe reductior vegetation moisture.

https://doi.org/10.5194/egusphere-2026-1902
Preprint. Discussion started: 14 April 2026

4 Results

In 2019, Brazil recorded the highest wildfire occurrence recorded in tropical regions of South America in the past two decades (Silva et al., 2021). In Peru, a marked increase in wildfire occurrence was documented in the Andean regions in 2016 (PCM, 2016; Zubieta et al., 2021b) and 2020 (Zubieta et al., 2023b). More recently, in 2024, a large number of wildfires overwhelmed the national government's response capacity (PCM, 2024a). To analyze wildfire hazard, a classification system was developed to estimate hazard levels in the Amazonian and Andean regions. Six wildfire hazard categories were defined: very low, low, moderate, high, very high, and extreme (Table 1).

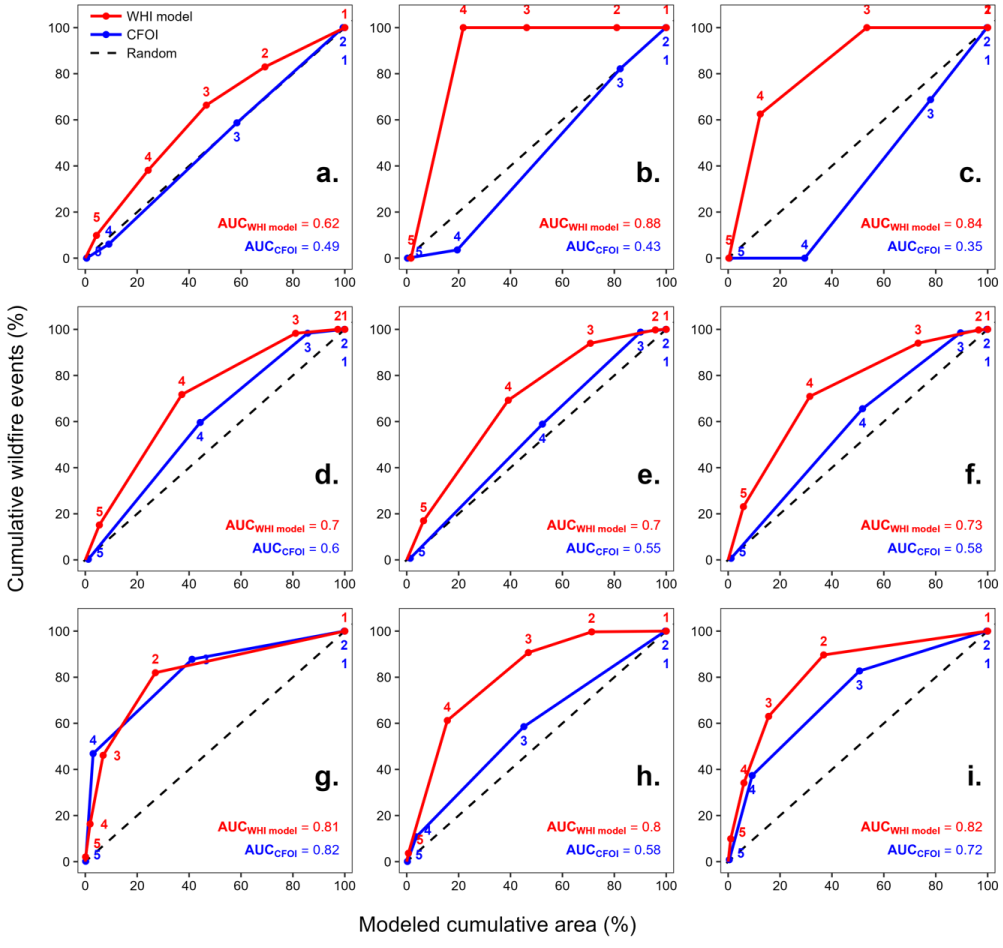

Figure 3: Success Rate Curves (SRC) for WHI and CFOI (MINAM, 2025) models, showing the Area Under the Curve (AUC). Hazard levels are referred to as: 1 (low), 2 (moderate), 3 (high), 4 (very high), 5 (extreme) for nine regions of Peru: a) North Coast (1), b) Central Coast (2), c) South Coast (3), d) Northern Andes (4), e) Central Andes (5), f) Southern Andes (6), g) Northern Amazon (7), h) Central Amazon (8), i) Southern Amazon (9). The location of the regions can be seen in Fig. 1.

Based on the best available data, to evaluate the model's temporal detection capability across hazard levels (on an 8-day timescale), wildfire events (defined as wildfire emergencies in Peru) were overlaid with the spatial distribution of hazard levels derived from the

https://doi.org/10.5194/egusphere-2026-1902
Preprint. Discussion started: 14 April 2026

model for the period May–December, 2019–2024 (Fig. 3). Figure 3 presents Success Rate Curves (SRC) illustrating the performance of the wildfire hazard model, using the Area Under the Curve (AUC). The AUC was estimated by comparing the cumulative percentage frequency of reported wildfire emergencies with the cumulative percentage frequency of the modeled surface area, calculated from the total number of pixels in the wildfire hazard index maps (generated every 8 days) during the study period. Hazard levels were grouped as follows: 1 (low), 2 (moderate), 3 (high), 4 (very high), and 5 (extreme), for the nine regions of Peru described in Figure 1.

The equidistribution line (dashed black line in Fig. 3) represents a scenario in which wildfire occurrences are uniformly distributed across space (hazard classes) and time (months). Results from the Index of Favorable Conditions for Fires in Vegetation (CFOI) provided by MINAM (2025) tend to be more evenly distributed in terms of wildfire occurrence (%) across hazard classes (%) compared to the WHI model proposed in this study (Fig. 3). SRC curves that closely follow the equidistribution line indicate limited model performance, as they fail to adequately capture the influence of key climatic, vegetation, and anthropogenic factors on wildfire hazard. This limitation is observed in the CFOI results for several Andean (Fig. 3d–f) and Amazonian regions of Peru (Fig. 3h). The central and southern coasts do not necessarily reflect optimal performance (Fig. 3a-c). The results of the proposed model exhibit a more heterogeneous detection pattern across both space and time (Fig. 3a–i). For example, approximately 20% of wildfire events recorded between 2019 and 2024 correspond to about 5–10% of the Andean region affected by extreme wildfire hazard (level 5) during drought periods (Fig. 3d–f). This pattern is consistent with years characterized by high wildfire frequency, such as 2020 (Zubieta et al., 2023b), and with 2024, when a state of emergency was declared because of the severity and frequency of wildfires (PCM, 2024b).

In the Andean region, the model primarily identifies level 5 (extreme hazard) as representative of seasonal periods with the highest wildfire occurrence, particularly during events that exceeded the response capacity of government agencies in 2024. In contrast, results for the Amazon region indicate that severe seasonal wildfire conditions are better captured by hazard levels 4 (very high) and 5 (extreme), as these categories encompass a larger proportion of wildfire events (Fig. 3g–i). For example, between 10% and 60% of wildfire events during 2019–2024 correspond to approximately 5–10% of the Amazonian region affected by high to extreme wildfire hazard (levels 4 and 5) during peak fire seasons (Fig. 3g–i).

To further examine the relationship between wildfire occurrence and modeled hazard, correlation coefficients were calculated between the number of wildfire events and the corresponding area associated with each hazard level (expressed as percentages) (Table 2). For comparison, the number of MODIS-derived hotspots was also analyzed relative to the modeled hazard area, and correlation coefficients were similarly computed for each hazard level (Table 2). The results indicate that correlations are generally not significant for hazard levels 1 (low), 2 (moderate), and 3 (high) across coastal, highland, and rainforest regions. However, the detection of extreme hazard (level 5) in the Andean and Amazonian regions shows greater consistency, with statistically significant correlations at the 90% and 95% confidence levels (Table 2).

https://doi.org/10.5194/egusphere-2026-1902
Preprint. Discussion started: 14 April 2026

Table 2: Correlation between percentage of reported events (using wildfires and hotspots) and percentage of surface area modeled for hazard level 1 (Low) , 2 (Moderate) , 3 (High), 4 (Very high) , 5 (Extreme) and 4+5 (Very high and Extreme) zones.

Region	Correlation coefficients - wildfires					
	r (level 1)	r (level 2)	r (level 3)	r (level 4)	r (level 5)	r (level 4+5)
North Coast	-	-	-	-	-	-
Central Coast	-	-	-	-	-	-
South Coast	-	-	-		-	-
Northern Andes	-	0.53	-	0.65	0.55	0.75
Central Andes	-	0.39	0.54	0.20	0.91	0.82
Southern Andes	0.45	-	-	0.54	0.90	0.79
Northern Amazon	0.13	-	-	0.71	-	0.78
Central Amazon	0.30	0.26	0.24	0.49	-	0.65
Southern Amazon	-	0.56	-	-	-	-
Region	Correlation coefficients - hotspots					
	r (level 1)	r (level 2)	r (level 3)	r (level 4)	r (level 5)	r (level 4+5)
North Coast	-	-	-	0.27	-	-
Central Coast	-	-	-	-	-	-
South Coast	-	-	-	0.23	-	-
Northern Andes	0.12	0.36	-	0.49	0.95	0.86
Central Andes		0.23	-	0.66	0.96	0.82
Southern Andes	0.52	-	0.46	0.41	0.94	0.70
Northern Amazon		0.41	0.55	0.86	-	-
Central Amazon	-	0.19	-	0.73	-	0.80
Southern Amazon	-	-	0.33	0.72	-	0.84

A notably high occurrence of wildfires was observed in 2020, 2022, and 2024, particularly in Andean and Amazonian regions (Fig. 4d–f). In contrast, model outputs for the coastal region do not exhibit a clear temporal pattern (Fig. 4a–c), suggesting limited performance in areas with sparse vegetation. This limitation may be associated with the extremely low precipitation conditions characteristic of the western slope of the Andes (Aybar et al., 2020). Compared to the coastal regions, where model performance is weaker (Fig. 4a–c), the proportion of wildfires reported within level 5 (extreme hazard) areas in the Andean region is consistent with the proportion of surface area classified as level 5 across six regions of Peru during 2019–2024 (Fig. 4d–f). Indeed, a strong and statistically significant correlation exists between the percentage of wildfire occurrence and the percentage of area classified as extreme hazard in the central ($r \approx 0.91$; $p < 0.01$) and southern Andes ($r \approx 0.90$; $p < 0.01$) (Table 2). These findings suggest that the model effectively captures periods of highest wildfire occurrence in Andean regions when extreme hazard levels are analyzed (Fig. 4d–f).

https://doi.org/10.5194/egusphere-2026-1902
Preprint. Discussion started: 14 April 2026

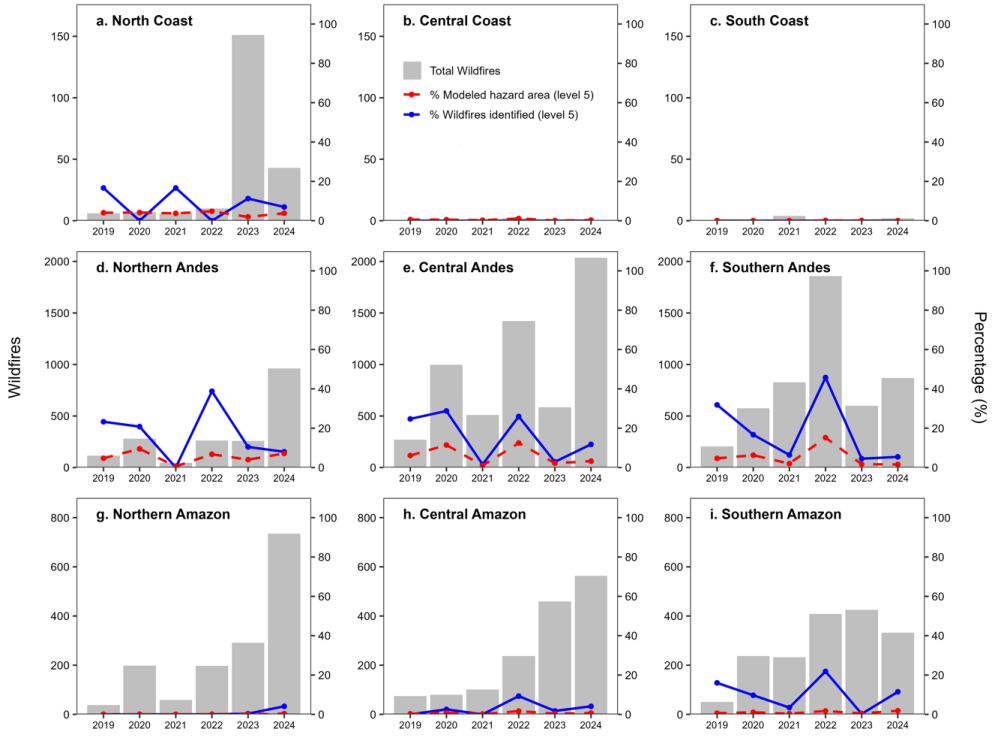

285 **Figure 4: Number of wildfires reported as emergency (gray bars). Percentage of wildfires reported and identified in modeled zones as level 5 (Extreme hazard level, blue line). Percentage of surface area (obtained from number of pixels) categorized as level 5 (red line) for nine regions of Peru: a) North Coast (1), b) Central Coast (2), c) South coast (3), d) Northern Andes (4), e) Central Andes (5), f) Southern Andes (6), g) Northern Amazon (7), h) Central Amazon (8), i) Southern Amazon (9). The location of the regions can be seen in Fig. 1.**

290 It is important to note that the exclusive use of extreme hazard (level 5) presents limitations in representing wildfire occurrence in Amazonian regions, as no clear relationship is observed between the two variables (Fig. 4g–i). To improve wildfire representation, hazard levels 4 (very high) and 5 (extreme) were jointly analyzed and proposed for Amazonian regions (Fig. 5a–i). The percentage of reported wildfires occurring within areas classified as levels 4 and 5 is consistent with the proportion of surface area categorized within these hazard levels, particularly in the central and northern Amazon (Fig. 5h–i) ($r \approx 0.78$; $p < 0.05$) (Table 2). These results suggest that
295 the proposed model can effectively represent and distinguish seasonal wildfire patterns in Amazonian regions when very high and extreme hazard levels are considered (Fig. 5h–i). Nevertheless, stronger model performance is observed in the Andean regions ($r \approx 0.78$; $p < 0.05$) (Table 2).

https://doi.org/10.5194/egusphere-2026-1902
Preprint. Discussion started: 14 April 2026

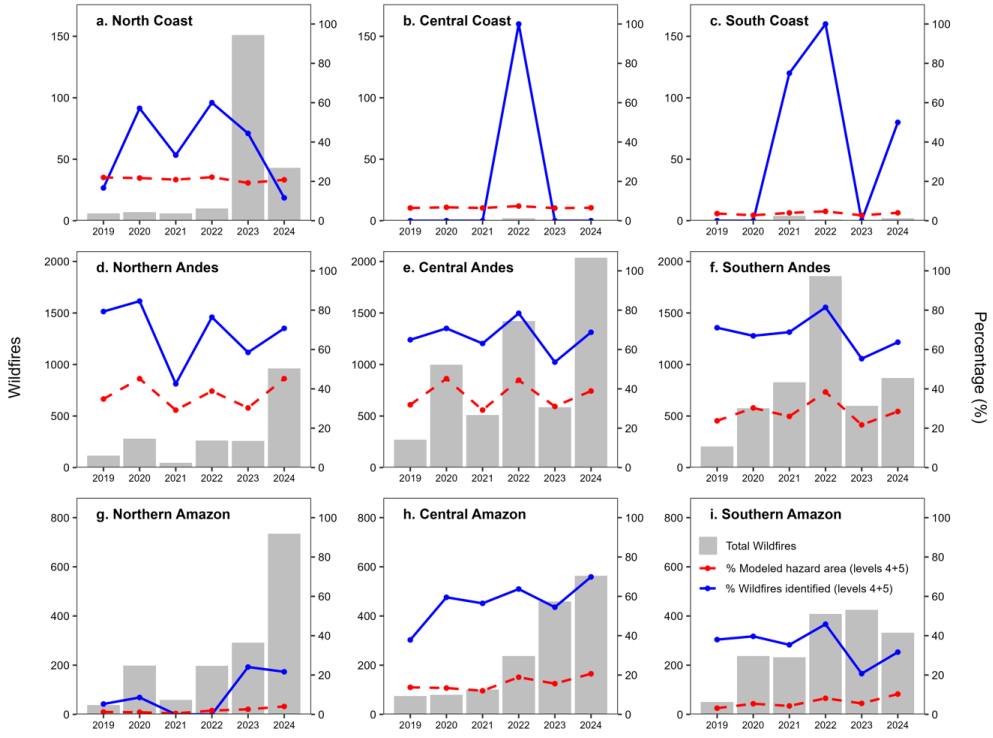

Figure 5: Number of wildfires reported as emergency (gray bars). Percentage of wildfires reported and identified in modeled zones as level 4 and 5 (Extreme hazard level, blue line). Percentage of surface area (obtained from number of pixels) categorized as level 4 and 5 (red line) for nine regions of Peru: a) North Coast (1), b) Central Coast (2), c) South coast (3), d) Northern Andes (4), e) Central Andes (5), f) Southern Andes (6), g) Northern Amazon (7), h) Central Amazon (8), i) Southern Amazon (9). The location of the regions can be seen in Fig. 1.

To further evaluate the model's ability to detect high-probability wildfire activity, MODIS-derived hotspots were incorporated into the analysis (Figs. 6 and 7). The results indicate that the proposed wildfire hazard model adequately captures the seasonal variability of hotspots between 2016 and 2024 when extreme hazard (level 5) is considered in Andean regions (Fig. 6d–f). A strong and statistically significant correlation is observed between the percentage of wildfire occurrence and the percentage of area classified as extreme hazard in the central Andean region ($r \approx 0.96$; $p < 0.05$) (Table 2). However, no clear temporal pattern is evident in Amazonian regions when only level 5 is considered (Fig. 6g–i).

https://doi.org/10.5194/egusphere-2026-1902
Preprint. Discussion started: 14 April 2026

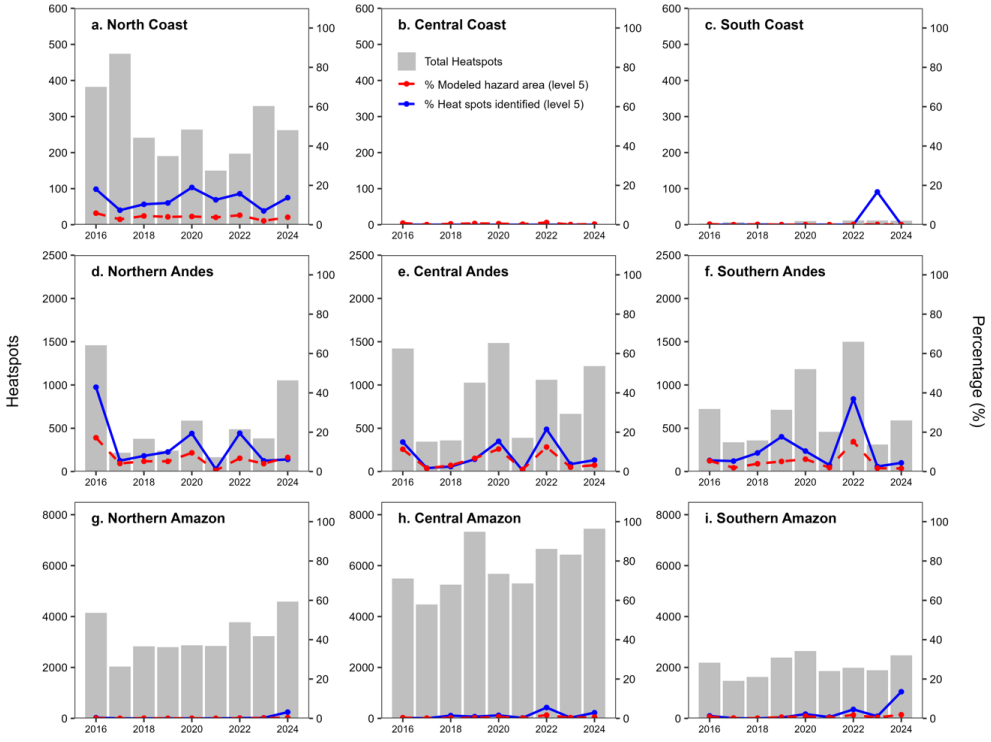

Figure 6: **Number of hotspots (gray bars). Percentage of hotspots identified in modeled zones as level 5 (Extreme hazard level, blue line). Percentage of surface area (obtained from number of pixels) categorized as level 5 (red line) for nine regions of Peru: a) North Coast (1), b) Central Coast (2), c) South Coast (3), d) Northern Andes (4), e) Central Andes (5), f) Southern Andes (6), g) Northern Amazon (7), h) Central Amazon (8), i) Southern Amazon (9). The location of the regions can be seen in Fig. 1.**

https://doi.org/10.5194/egusphere-2026-1902
Preprint. Discussion started: 14 April 2026

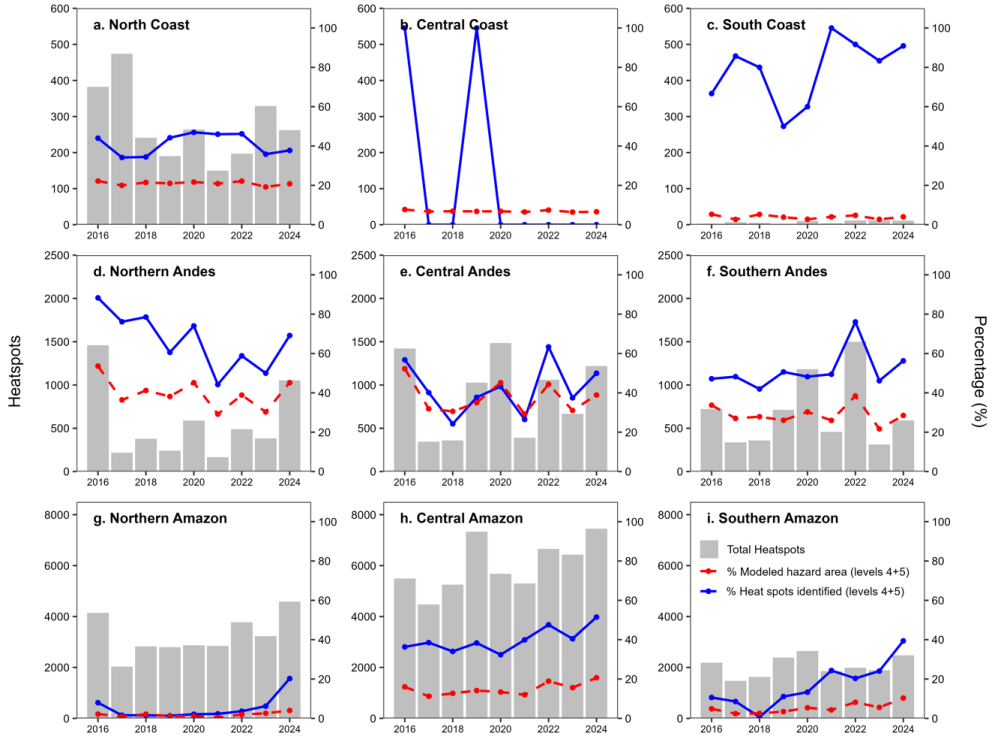

Figure 7: Number of hotspots (gray bars). Percentage of hotspots identified in modeled zones as level 4 and 5 (Extreme hazard level, blue line). Percentage of surface area (obtained from number of pixels) categorized as level 4 and 5 (red line) for nine regions of Peru: a) North Coast (1), b) Central Coast (2), c) South Coast (3), d) Northern Andes (4), e) Central Andes (5), f) Southern Andes (6), g) Northern Amazon (7), h) Central Amazon (8), i) Southern Amazon (9). The location of the regions can be seen in Fig. 1.

To enhance the analysis in these regions, the percentage of MODIS hotspots occurring within areas classified as very high and extreme hazard (levels 4 and 5) was also evaluated (Fig. 7). The results suggest that in Amazonian regions, the combined use of hazard levels 4 and 5 is more appropriate for identifying periods of increased wildfire risk (Fig. 7g–i), although detection remains less robust than in the Andes. Improved consistency between wildfire occurrence and model outputs is observed when both hazard levels are considered, particularly in the central ($r \approx 0.80$; $p < 0.01$) and southern Amazon regions of Peru ($r \approx 0.84$; $p < 0.01$) (Table 2). For preventive purposes, this study proposes a set of optimized parameters (w_n) for monitoring wildfire hazard in the Andean and Amazonian regions (Table 3).

https://doi.org/10.5194/egusphere-2026-1902
Preprint. Discussion started: 14 April 2026

335

Table 3: Optimized parameters (w_n), Area Under the Curve (AUC), and correlation coefficients between the percentage of modeled area (levels 5 and 4+5) and the percentage of wildfires and hotspots for the periods 2019–2024 and 2002–2024, respectively.

Region	Wa	Wb	Wc	Wd	AUC	Wildfire		Hotspots	
						(5)	(4+5)	(5)	(4+5)
North Coast	0.10	0.10	0.60	0.20	0.62	-		0.79	0.49
Central Coast	0.15	0.15	0.50	0.20	0.88	-	-	-	-
South Coast	0.15	0.15	0.20	0.50	0.84	-	0.89	-	0.04
Northern Andes	0.10	0.40	0.10	0.40	0.70	0.55	0.75	0.92	0.86
Central Andes	0.15	0.50	0.15	0.20	0.70	0.91	0.82	0.96	0.82
Southern Andes	0.20	0.40	0.20	0.20	0.73	0.90	0.79	0.95	0.61
Northern Amazon	0.10	0.60	0.15	0.15	0.81	0.94	0.78	0.93	0.86
Central Amazon	0.15	0.15	0.50	0.20	0.80	0.97	0.65	0.94	0.87
Southern Amazon	0.10	0.60	0.15	0.15	0.82	0.64	-	0.84	0.86

340 The results indicate that the Andean region and the Andean–Amazon transition zone (1500–4000 m above sea level) are primarily exposed to extreme levels of forest fire danger at the onset of the rainy season (November) along the Andes (Fig. 8a). A similar spatial pattern of extreme fire danger is also observed at the end of the dry season, or period of minimal rainfall (September), across both Andean and Amazonian regions (Fig. 8b).

345

350

355

https://doi.org/10.5194/egusphere-2026-1902
Preprint. Discussion started: 14 April 2026

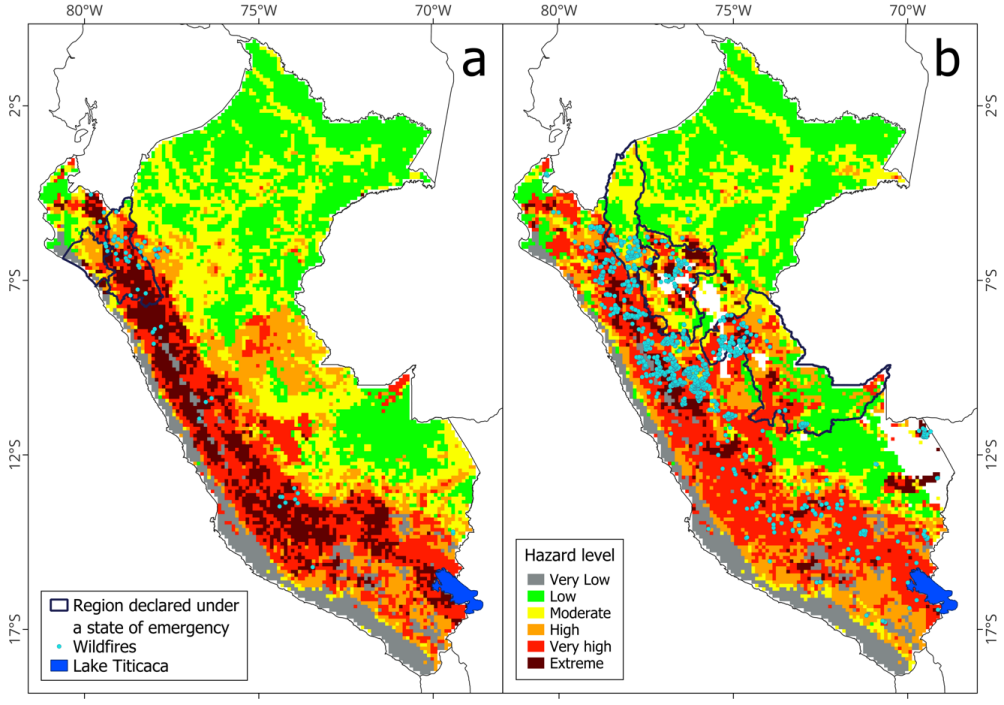

Figure 8: Wildfire Hazard Index (WHI) for (a) 16–23 November 2026 and (b) 13–20 September 2024, corresponding to periods during which states of emergency for wildfires were declared by the Government of Peru.

In Peru, a marked increase in wildfire activity was identified in 2016 (Zubieta et al., 2021b) and 2024. These conditions were reflected in the declaration of states of emergency due to wildfires across multiple regions during these years (PCM, 2016, 2024a). Wildfire hazard across Peru is adequately represented by the model when very high and extreme WHI levels (Levels 4 and 5, respectively) are analyzed (Fig. 8), as these categories correspond to critical vegetation conditions that are key determinants of fuel dryness and wildfire occurrence (Zubieta et al., 2021b; IGP, 2024).

5 Discussion

Short-term wildfire hazard or risk indices are typically developed using variables associated with climatic conditions—such as temperature, relative humidity, wind speed, and precipitation (McArthur, 1967a; Van Wagner, 1974, 1987)—or parameters that reflect the influence of climate on vegetation and fuel characteristics (Goodrick, 2002; Sharples et al., 2009). However, these methodologies are often region-specific and are not necessarily transferable to other areas, as wildfire regimes vary according to local environmental and climatic conditions (Adab et al., 2013; Castel-Clavera et al., 2025; Srock et al., 2018). Consequently, wildfire hazard indices must be adapted to the specific characteristics of each region, particularly in countries with high biodiversity and diverse climatic regimes, such as Peru.

https://doi.org/10.5194/egusphere-2026-1902
Preprint. Discussion started: 14 April 2026

In response, numerous studies worldwide have incorporated satellite data to better capture the role of vegetation in terms of moisture content and its influence on wildfire occurrence (Chen et al., 2023; Chowdhury and Hassan, 2013; Chuvieco et al., 2004; Laneve et al., 2020; Yebra et al., 2013). Satellite observations enable the characterization of the spatial and temporal variability of vegetation responses to precipitation (Asner et al., 2017; Brieva et al., 2023). In this context, this study proposes a new wildfire hazard index for the Amazonian and Andean regions of Peru, integrating observational data with satellite-derived products such as GPM (Huffman et al., 2023) and MODIS (Vermote et al., 2002).

To enhance the performance of wildfire hazard indices, recent approaches have also incorporated factors related to ignition sources and anthropogenic influences (Adab et al., 2013; Bisquert et al., 2014; Di Giuseppe et al., 2025). Accordingly, the wildfire hazard model developed in this study integrates datasets representing fuel characteristics (MINAM, 2019) and cultivated areas across Peru to account for human-induced fire activity.

The regional variability in optimal weighting scenarios reflects the ecological heterogeneity of the Peruvian territory. On the North Coast and in the Central Amazon, the anthropogenic component presents the highest weights, reflecting the predominant role of slash-and-burn agricultural practices as the main ignition source (Alvarez et al., 2025; Taboada-Hermoza & Martínez, 2025). In the Andean regions, vegetation conditions and fuel load concentrate the highest weights, with high-altitude grasslands representing the structural component that determines the baseline hazard level, while vegetation water stress acts as a dynamic modulator during drought episodes (Zubieta et al., 2021b; Ccanchi, 2021). In the Northern and Southern Amazon, the dominance of vegetation conditions indicates that seasonal phenological dynamics are the main predictor of wildfire hazard in these ecosystems.

The results indicate that the model does not adequately capture the spatial or temporal patterns of wildfire hazard in coastal regions (below 1500 masl). This limitation suggests reduced model performance in areas dominated by sparse vegetation and prolonged dry periods without rainfall. Although the coastal region lies within tropical South America, it is characterized by arid conditions, with precipitation occurring mainly during El Niño events, when extreme rainfall conditions may develop (Woodman and Takahashi, 2014). The results of the wildfire hazard model proposed in this study demonstrate an adequate capability to detect the seasonal occurrence of wildfires between 2019 and 2024 when extreme hazard levels are considered in Andean mountain regions. However, the Amazonian region is not adequately represented when only extreme hazard (level 5) is analyzed. To improve hazard assessment in Amazonian areas, the combined use of hazard levels 4 and 5 (very high and extreme) is recommended.

Extreme environmental conditions—such as high temperatures and reduced precipitation—play a critical role in altering vegetation and are key determinants of fuel conditions and wildfire occurrence (Chen et al., 2023). In Peru, such conditions are reflected in the declaration of (a) states of emergency due to wildfires in multiple regions (PCM, 2016, 2024a), and (b) states of emergency due to water deficits associated with prolonged dry periods (PCM, 2024b).

The results indicate that the hazard model is also effective in representing fire activity, as reflected by thermal anomalies (hotspots) derived from MODIS satellite data, at both regional and national scales. Hotspots are particularly useful for characterizing fire activity when burned areas range between 50 and 100 hectares in Andean zones (Zubieta et al., 2023a). The findings show a consistent detection of seasonal hotspot patterns between 2016 and 2024, particularly under very high and extreme wildfire hazard conditions in both Amazonian and Andean regions. For operational wildfire monitoring, the use of satellite data—given its high spatial and temporal resolution—combined with hotspot observations, provides a valuable tool for continuous validation and improvement of hazard models.

https://doi.org/10.5194/egusphere-2026-1902
Preprint. Discussion started: 14 April 2026

The spatial distribution of the WHI indicates that extreme hazard is primarily associated with higher vegetation loads in Andean forests (PCM, 2016; MINAM, 2019) and Andean–Amazonian forests (PCM, 2024a; MINAM, 2019), consistent with emergency declarations triggered by increases in difficult-to-control wildfires in 2016 and 2024. The spatial extent of extreme hazard identified by the WHI model for November 2016 along the Andes may be attributed to a prolonged dry season, or a period of below-normal rainfall lasting between 5 and 7 months, as documented for Andean and Amazonian regions of South America (Jimenez et al., 2021). A similar scenario of extreme hazard was observed in September 2024, characterized by a high number of wildfires, during which the dry season in Amazonian regions of Peru extended until November 2024 (IGP, 2024b), also leading to the declaration of a state of emergency due to water scarcity in November 2024 (PCM, 2024b). These findings suggest that the effectiveness of wildfire hazard alerts based on the WHI model proposed in this study is closely linked to the accurate estimation of the duration and severity of meteorological drought in the Andean and Amazonian regions.

The wildfire hazard model proposed in this study has the potential to contribute to the development of wildfire prevention systems in Peru, where such systems remain limited. Existing wildfire information systems, whether developed by governmental agencies (Araújo et al., 2025) or researchers, are typically based on hazard or risk indices (Delgado et al., 2022; Ziccardi et al., 2020). For example, the Canadian Forest Fire Danger Rating System is based on the Fire Weather Index (FWI) (Forestry Canada, 1992; Van Wagner, 1987). In South America, Argentina uses the Forest Fire Danger Index (CONAE, 2026), derived from the Australian system developed by McArthur (1967), while Brazil uses the Nesterov Ignition Index (INM, 2026), a cumulative index for classifying wildfire danger on a daily basis (Nesterov, 1949).

In the context of climate change and evolving drought regimes, wildfires are likely to pose an increasing threat to tropical ecosystems in the coming decades (González et al., 2025). As in other regions of South America, where climatic patterns strongly influence fire activity (Silva et al., 2025), the seasonal increase in wildfire frequency in the Andean–Amazonian region of Peru is being modulated and intensified by the frequency, duration, and severity of drought periods (Zubieta et al., 2021b, 2023b). Operational monitoring of vegetation dynamics and drought impacts is therefore essential, as these factors directly influence the seasonal and intra-seasonal variability of wildfire hazard.

An important avenue for improving hazard prediction models lies in the application of artificial intelligence techniques. In this context, data quality should be prioritized, as it is fundamental to achieving significant advances in fire activity forecasting, particularly regarding the spatial and temporal dynamics of forest fuel (Andrianarivony and Akhloufi, 2024). Indeed, data quality may be more critical than model complexity in enhancing the predictive performance of artificial intelligence approaches applied to wildfire hazard (Di Giuseppe et al., 2025).

5.1 Uncertainty of this study

Although wildfire location data in Peru are approximate and primarily based on emergency reports (MINAM, 2025), their spatial and temporal distribution was used to evaluate the performance of the model in identifying wildfire hazard levels. The model relies on a climatic variable that is highly relevant for Andean regions, as demonstrated by Zubieta et al. (2021b), but not necessarily applicable to Amazonian regions. Nevertheless, calibration of model coefficients through a sensitivity analysis approach made it possible to classify hazard functions at a regional scale using the Wildfire Hazard Index (WHI). The results indicate that model performance varies across regions when coastal, Andean, and Amazonian zones are analyzed independently. The application of region-specific functions,

https://doi.org/10.5194/egusphere-2026-1902
Preprint. Discussion started: 14 April 2026

as proposed in this study, is therefore recommended to achieve optimal performance in Andean and Amazonian regions. This variability reflects the influence of fuel load across diverse ecosystems in South America (Fearnside, 2017), particularly in Peru, which exhibits high ecological diversity across its coastal, Andean, and Amazonian regions (Pulgar Vidal, 2014).

The findings indicate that the model can adequately represent the probability of wildfire occurrence reported as emergencies (extreme hazard level), achieving an approximate efficiency of 80% in Andean regions. However, model performance in Amazonian regions is not adequate; when very high and extreme hazard levels are analyzed jointly, model performance improves to approximately 60% for these areas.

It is important to note that wildfire events reported by civil defense authorities are typically concentrated near roads and rivers (Zubieta et al., 2023a), suggesting that fire activity in remote or high-altitude regions may be underreported. Satellite-derived fire activity data provide a valuable complementary source for evaluating wildfire hazard models at local and regional scales in Amazonian areas, where official records are limited. Indeed, model performance increases slightly (to approximately 64%) when analyzing the occurrence of thermal anomalies (hotspots) within areas classified as very high and extreme hazard in Amazonian regions. This suggests that the model is able to adequately identify wildfire hazard in these regions when both hazard levels are considered simultaneously.

The use of Dry-Day Frequency and NDVI, derived from remote sensing data, enables the detection of dynamic changes in rainfall deficits and vegetation conditions, respectively. In addition, a static variable representing fuel type (i.e., forests, shrublands, and grasslands) was incorporated to characterize combustible material. However, the primary ignition source in this region of South America is associated with fire use in agricultural and livestock activities (Alvarez et al., 2025; Roman et al., 2024; Taboada-Hermoza and Martínez, 2025). In the current model, this anthropogenic factor is represented at the national scale solely through agricultural planting areas, which may be a limitation, as it does not account for (a) the quantity and type of crop residues following land clearing, (b) the use of fire for pasture renewal, and (c) variations in fire use within protected natural areas.

Beyond computational capacity and data availability, the selection of wildfire hazard models should be guided by region-specific characteristics (Ejaz and Choudhury, 2025). In this context, potential improvements to model performance at regional and local scales may include (a) incorporating crop type and phenological stages, and (b) integrating the spatial and temporal history of wildfires associated with controlled burns in livestock systems and protected areas. Recent advances also highlight the potential of machine learning and deep learning approaches for wildfire hazard assessment (Ejaz and Choudhury, 2025; He et al., 2024; Ismail et al., 2024; Xu et al., 2025).

6 Conclusions

The increasing frequency of wildfires in South America has been closely linked to climatic factors, particularly drought. In Peru, wildfires are commonly associated with uncontrolled burning practices in agricultural and livestock activities. To reduce the likelihood of such burns developing into wildfires, continuous monitoring of wildfire hazard is essential. Accurate prediction of wildfire hazard is therefore critical for enhancing the safety of local populations and firefighters. In this study, a Wildfire Hazard Index (WHI) was developed based on Dry-Day Frequency (DDF), the Normalized Difference Vegetation Index (NDVI), cultivated area (CA), and forest fuel (FF). The proposed method enables the assessment of short-term wildfire hazard (8-day intervals) in the Amazonian and Andean regions of Peru, where these indicators are often limited or unavailable. The input variables—NDVI, DDF, FF, and CA—are identified

https://doi.org/10.5194/egusphere-2026-1902
Preprint. Discussion started: 14 April 2026

as key parameters for analyzing wildfire hazard levels. The results demonstrate consistency between WHI outputs and fire activity, as represented by reported wildfire emergencies and satellite-derived hotspots. The analysis suggests that the model adequately captures the seasonal variability of wildfire hazard. This indicates that the proposed method can support hazard classification and contribute to the development of regional wildfire early warning systems in the Amazonian and Andean regions. It can also be applied to generate short- and medium-term seasonal forecasts of wildfire hazard, contributing to disaster risk management by governmental institutions. Finally, the integration of machine learning and deep learning approaches is recommended to further enhance the generation of wildfire hazard maps in Andean–Amazonian regions.

Author contributions.

YC developed the framework, conducted the experiments, and analyzed the data under the supervision of RZ. YC also provided international datasets and guided their processing, including the processing of satellite datasets and Peruvian fire datasets. YC, JP, and JS contributed to the code development and provided guidance for the WHI calculations. RZ contributed domain expertise for the interpretation of the results and led the writing of the manuscript. All authors contributed to shaping the research, analysis, and final manuscript.

Competing interests.

The contact author has declared that none of the authors has any competing interests.

Acknowledgments

The authors would like to thank The Fire Information for Resource Management System (FIRMS) for providing hotspot datasets. The authors also acknowledge the NASA Goddard Earth Sciences (GES) Data and Information Services Center (DISC) for providing GPM-IMERG [https://jsimpsonhttps.pps.eosdis.nasa.gov/imerg/gis/] datasets. Ricardo Zubieta would like to express his gratitude to the Ministry of Environment and Ministry of Development, Agriculture and Irrigation for providing the wildfire and agricultural datasets, respectively.

Financial support

The authors would like to thank to PP068 (Budget program of Peru: Reduction of vulnerability and attention to emergencies due to disasters). Suggestions from B. Fraser were also greatly appreciated. This paper was funded by the National Council of Science, Technology and Technological Innovation (CONCYTEC) and the National Program for Scientific Research and Advanced Studies (PROCIENCIA) within the framework of the competition “E041-2024-03 Basic Research Projects” [contract number PE501088039-2024].

https://doi.org/10.5194/egusphere-2026-1902
Preprint. Discussion started: 14 April 2026

References

Acevedo Ortiz, M. Y., Arias Gómez, P. A., and Villa Garzón, F. A.: Sequías e incendios forestales en América Latina: una revisión sistemática de literatura, Colomb. For., 29, e23266, https://doi.org/10.14483/2256201X.23266, 2026.

Adab, H., Kanniah, K. D., and Solaimani, K.: Modeling forest fire risk in the northeast of Iran using remote sensing and GIS techniques, Nat. Hazards, 65, 1723–1743, https://doi.org/10.1007/s11069-012-0450-8, 2013.

Adaktylou, N., Stratoulias, D., and Landenberger, R.: Wildfire Risk Assessment Based on Geospatial Open Data: Application on Chios, Greece, ISPRS Int. J. Geo-Information, 9, 516, https://doi.org/10.3390/ijgi9090516, 2020.

Alcarde Alvares, C., Cegatta, I., Vieira, L., Freitas Pavani, R., de Mattos, E., Sentelhas, P., Stape, J., and Soares, R.: Forest fire danger: Application of Monte Alegre Formula and assessment of the historic for Piracicaba, SP, Sci. For. Sci., 42, 521–532, 2014.

Alvarez, S., Martínez, A. G., Zubieta, R., and Ccanchi, Y.: Rethinking the agricultural use of fire and its influence on the occurrence of wildfire in high Andean communities of Cusco, Peru, Int. J. Disaster Risk Reduct., 128, 105702, https://doi.org/10.1016/j.ijdrr.2025.105702, 2025.

Ambadan, T., Oja, M., Gedalof, Z., and Berg, A. A.: Satellite-Observed Soil Moisture as an Indicator of Wildfire Risk, Remote Sens., 12, https://doi.org/10.3390/rs12101543, 2020.

Andrianarivony, H. S. and Akhloufi, M. A.: Machine Learning and Deep Learning for Wildfire Spread Prediction: A Review, Fire, 7, https://doi.org/10.3390/fire7120482, 2024.

Araújo, T., Almeida, D., Sobral, I., Brasil, H., Trevisan, E., Sales, A., Soares, A., and Filho, J.: Real-Time Monitoring System for Forest Fire Prevention and Combat: A Case Study in the Brazilian Semi-Arid Region, 270–279, https://doi.org/10.5753/sbsi.2025.246473, 2025.

Artés, T., Castellnou, M., Houston Durrant, T., and San-Miguel, J.: Wildfire--atmosphere interaction index for extreme-fire behaviour, Nat. Hazards Earth Syst. Sci., 22, 509–522, https://doi.org/10.5194/nhess-22-509-2022, 2022.

Asner, G. P., Martin, R. E., Tupayachi, R., and Llactayo, W.: Conservation assessment of the Peruvian Andes and Amazon based on mapped forest functional diversity, Biol. Conserv., 210, 80–88, https://doi.org/10.1016/j.biocon.2017.04.008, 2017.

Aybar, C., Fernández, C., Huerta, A., Lavado, W., Vega, F., and Felipe-Obando, O.: Construction of a high-resolution gridded rainfall dataset for Peru from 1981 to the present day, Hydrol. Sci. J., 65, 770–785, https://doi.org/10.1080/02626667.2019.1649411, 2020.

Bax, V. and Francesconi, W.: Conservation gaps and priorities in the Tropical Andes biodiversity hotspot: Implications for the expansion of protected areas, J. Environ. Manage., 232, 387–396, https://doi.org/10.1016/j.jenvman.2018.11.086, 2019.

Bisquert, M., Sánchez, J. M., and Caselles, V.: Modeling Fire Danger in Galicia and Asturias (Spain) from MODIS Images, Remote Sens., 6, 540–554, https://doi.org/10.3390/rs6010540, 2014.

Bountzouklis, C., Fox, D. M., and Bernardino, E. Di: Predicting wildfire ignition causes in Southern France using eXplainable Artificial Intelligence (XAI) methods, Environ. Res. Lett., 18, 44038, https://doi.org/10.1088/1748-9326/acc8ee, 2023.

Bradshaw, L. S., Deeming, J. E., Burgan, R. E., and Cohen, J. D.: The 1978 National Fire-Danger Rating System: technical documentation, https://doi.org/10.2737/INT-GTR-169, 1984.

Brieva, C., Saco, P. M., Sandi, S. G., Mora, S., and Rodríguez, J. F.: NDVI Response to Satellite-Estimated Antecedent Precipitation in Dryland Pastures, Remote Sens., 15, 3615, https://doi.org/10.3390/rs15143615, 2023.

https://doi.org/10.5194/egusphere-2026-1902
Preprint. Discussion started: 14 April 2026

Burgan, R. E.: 1988 Revisions to the 1978 National Fire-Danger Rating System. USDA Forest Service Research Paper INT USA. SE-273, http://www.floresta.ufpr.br/firelab/artigos/artigo370.pdf, 1988.

Camargo Caicedo, Y., Bolaño-Diaz, S., Pomares-Meza, G. M., Pérez-Pérez, M., Soro, T. D., Bolaño-Ortiz, T. R., and Vélez-Pereira, A. M.: Hydroclimatic and Land Use Drivers of Wildfire Risk in the Colombian Caribbean, Fire, 8, 221, https://doi.org/10.3390/fire8060221, 2025.

Carta, F., Zidda, C., Putzu, M., Loru, D., Anedda, M., and Giusto, D.: Advancements in Forest Fire Prevention: A Comprehensive Survey, Sensors, 23, https://doi.org/10.3390/s23146635, 2023.

Castel-Clavera, J., Pimont, F., Opitz, T., Ruffault, J., Barbero, R., Allard, D., and Dupuy, J.-L.: A comparative analysis of fire-weather indices for enhanced fire activity prediction with probabilistic approaches, Agric. For. Meteorol., 361, 110315, https://doi.org/10.1016/j.agrformet.2024.110315, 2025.

Ccanchi, Y.: Evaluación de sequías y del riesgo potencial a la ocurrencia de incendios forestales en ecosistemas altoandinos mediante uso de sensores remotos, https://repositorio.lamolina.edu.pe/handle/20.500.12996/5195, 2021.

Ccanchi, Y., & Zubieta, R. (2024). Monitoreo de fuegos activos en Áreas Naturales Protegidas del Perú a partir de datos de sensoramiento remoto. *Boletín científico El Niño, Instituto Geofísico del Perú, 11* (10), 12-18. https://repositorio.igp.gob.pe/items/6a631179-156d-43b4-b9e8-ac142a9caddc

CENEPRED: Escenario de riesgo por incendios forestales, http://sigrid.cenepred.gob.pe/sigridv3/storage/biblioteca//10471_escenario-de-riesgo-por-incendios-forestales.pdf, 2020.

Chandler, C., Cheney, P., Thomas, P., Trabaud, L., and Williams, D.: Fire in forestry. v.1: Forest fire behavior and effects. - v. 2: Forest fire management and organization, Food Agric. Organ. United Nations, 1983.

Chen, C., Xu, T., Sun, F., and Zhao, D.: A fire danger index assessment method for short-term pre-warning of wildfires: A case study of Xiangxi, China, Saf. Sci., 167, 106287, https://doi.org/10.1016/j.ssci.2023.106287, 2023.

Chowdhury, E. H. and Hassan, Q. K.: Use of remote sensing-derived variables in developing a forest fire danger forecasting system, Nat. Hazards, 67, 321–334, https://doi.org/10.1007/s11069-013-0564-7, 2013.

Chuvieco, E., Cocero, D., Riaño, D., Martin, P., Martínez-Vega, J., de la Riva, J., and Pérez, F.: Combining NDVI and surface temperature for the estimation of live fuel moisture content in forest fire danger rating, Remote Sens. Environ., 92, 322–331, https://doi.org/10.1016/j.rse.2004.01.019, 2004.

CONAE: Pronóstico de Índice de Riesgo de Incendio. Comisión Nacional de Actividades Espaciales, https://www.argentina.gob.ar/ciencia/conae/aplicaciones-de-la-informacion-satelital/pronostico-de-indice-riesgo-de-incendio, 2026.

Cubas, F. H.: Sectorización Climatica Del Territorio Peruano. Subdirección de Predicción Climática de la DMA. Servicio Nacional de Meteorología e Hidrología del Perú, https://repositorio.senamhi.gob.pe/handle/20.500.12542/976?locale-attribute=en, 2021.

Delgado, R. C., Wanderley, H. S., Pereira, M. G., Almeida, A. Q. de, Carvalho, D. C. de, Lindemann, D. da S., Zonta, E., Menezes, S. J. M. da C. de, Santos, G. L. dos, Santana, R. O. de, Souza, R. S. de, and Santos, O. A. Q. dos: Assessment of a New Fire Risk Index for the Atlantic Forest, Brazil, Forests, 13, 1844, https://doi.org/10.3390/f13111844, 2022.

https://doi.org/10.5194/egusphere-2026-1902
Preprint. Discussion started: 14 April 2026

Ejaz, N. and Choudhury, S.: A comprehensive survey of the machine learning pipeline for wildfire risk prediction and assessment, Ecol. Inform., 90, 103325, https://doi.org/10.1016/j.ecoinf.2025.103325, 2025.

Espinoza, J. C., Ronchail, J., Guyot, J. L., Junquas, C., Drapeau, G., Martinez, J. M., Santini, W., Vauchel, P., Lavado, W., Ordoñez, J., and Espinoza, R.: From drought to flooding: understanding the abrupt 2010–11 hydrological annual cycle in the Amazonas River and tributaries, Environ. Res. Lett., 7, 24008, https://doi.org/10.1088/1748-9326/7/2/024008, 2012.

Espinoza, J. C., Segura, H., Ronchail, J., Drapeau, G., and Gutierrez-Cori, O.: Evolution of wet-day and dry-day frequency in the western Amazon basin: Relationship with atmospheric circulation and impacts on vegetation, Water Resour. Res., 52, 8546–8560, https://doi.org/10.1002/2016WR019305, 2016.

Espinoza, J. C., Segura, H., Ronchail, J., Drapeau, G., and Gutierrez-Cori, O.: Evolution of wet-day and dry-day frequency in the western <scp>A</scp> mazon basin: Relationship with atmospheric circulation and impacts on vegetation, Water Resour. Res., 52, 8546–8560, https://doi.org/10.1002/2016WR019305, 2016.

Espinoza Villar, J. C., Ronchail, J., Guyot, J. L., Cochonneau, G., Naziano, F., Lavado, W., De Oliveira, E., Pombosa, R., and Vauchel, P.: Spatio-temporal rainfall variability in the Amazon basin countries (Brazil, Peru, Bolivia, Colombia, and Ecuador), Int. J. Climatol., 29, 1574–1594, https://doi.org/10.1002/joc.1791, 2009.

Eugenio, F. C., dos Santos, A. R., Fiedler, N. C., Ribeiro, G. A., da Silva, A. G., dos Santos, Á. B., Paneto, G. G., and Schettino, V. R.: Applying GIS to develop a model for forest fire risk: A case study in Espírito Santo, Brazil, J. Environ. Manage., 173, 65–71, https://doi.org/10.1016/j.jenvman.2016.02.021, 2016.

Fadrique, B., Costa, F., Cuesta, F., Arellano, G., Cayuela, L., Baker, T. R., Draper, F. C., Esquivel-Muelbert, A., ter Steege, H., Bauters, M., Aguirre-Gutiérrez, J., Aguirre-Mendoza, Z., Alexiades, M. N., Alvarez-Davila, E., Arets, E., Ayala, E., Aymard, C. G. A., Baccaro, F., Báez, S., Baraloto, C., Barbosa, R. I., Barbosa Camargo, P., Barlow, J., Barni, P. E., Barroso, J., Benchimol, M., Bennett, A. C., Berenguer, E., Blanc, L., Bonal, D., Bongers, F., Brienen, R., Brown, F., BT Andrade, M., Burban, B., Burnham, R. J., Camargo, J. L., Carvalho, S. P. C., Castilho, C., Chave, J., Coelho de Souza, F., Comiskey, J., da Costa, L., de Lima, R. B., de Oliveira, E. A., de Oliveira, R. L. C., de Oliveira Perdiz, R., De Rutte, J., del Aguila-Pasquel, J., Derroire, G., Di Fiore, A., Disney, M., Duque, A., Emilio, T., Farfan-Rios, W., Fauset, S., Fearnside, P. M., Feeley, K. J., Feldpausch, T. R., Ferreira, J., Ferreira, L., Flores Llampazo, G. R., Galbraith, D., García-Cabrera, K., García Criado, M., Gloor, E., Grandez-Rios, J. M., Hérault, B., Homeier, J., Honorio Coronado, E. N., Huamantupa-Chuquimaco, I., Huaraca Huasco, W., Huillca-Aedo, Y. T., Idárraga, Á., Jadán-Maza, O., Kalamandeen, M., Killeen, T. J., Laurance, S. G. W., Laurance, W. F., Levesley, A., Lopez, W., Macía, M. J., Magnusson, W. E., Malhi, Y., Manzatto, A. G., Marimon, B. S., Marimon Junior, B. H., Martínez-Villa, J. A., Medeiros, M. B., Melgaço, K., Melo, L., Metzker, T., Monteagudo, A., Morandi, P. S., Myers, J. A., Nascimento, H. M., Nascimento, R., Neill, D., Nieto-Ariza, B., et al.: Tree diversity is changing across tropical Andean and Amazonian forests in response to global change, Nat. Ecol. Evol., 10, 267–280, https://doi.org/10.1038/s41559-025-02956-5, 2026.

Fearnside, P. M.: South American Natural Ecosystems, Status of ☆, in: Reference Module in Life Sciences, Elsevier, https://doi.org/10.1016/B978-0-12-809633-8.02224-X, 2017.

Fernandes, P. M.: Combining forest structure data and fuel modelling to classify fire hazard in Portugal, Ann. For. Sci., 66, 415, https://doi.org/10.1051/forest/2009013, 2009.

Forestry Canada, F.: Development and structure of the Canadian Forest Fire Behavior Prediction System. Forestry Canada, https://www.frames.gov/documents/catalog/forestry_canada_fire_danger_group_1992.pdf, 1992.

https://doi.org/10.5194/egusphere-2026-1902
Preprint. Discussion started: 14 April 2026

Gajardo, J., Yáñez, M., Padilla, R., Espinoza, S., and Carrasco-Benavides, M.: Modeling the Spatial Distribution of Wildfire Risk in Chile Under Current and Future Climate Scenarios, Fire, 8, https://doi.org/10.3390/fire8030113, 2025.

Geirinhas, J. L., Russo, A. C., Libonati, R., Miralles, D. G., Ramos, A. M., Gimeno, L., and Trigo, R. M.: Combined large-scale tropical and subtropical forcing on the severe 2019–2022 drought in South America, npj Clim. Atmos. Sci., 6, 185, https://doi.org/10.1038/s41612-023-00510-3, 2023.

Giglio, L., Boschetti, L., Roy, D. P., Humber, M. L., and Justice, C. O.: The Collection 6 MODIS burned area mapping algorithm and product, Remote Sens. Environ., 217, 72–85, https://doi.org/10.1016/j.rse.2018.08.005, 2018.

Di Giuseppe, F., McNorton, J., Lombardi, A., and Wetterhall, F.: Global data-driven prediction of fire activity, Nat. Commun., 16, 2918, https://doi.org/10.1038/s41467-025-58097-7, 2025.

González, T. M., González-Trujillo, J. D., Elizalde, M. M., and Armenteras, D.: Predicting fire risk in colombia tropical savannas: A multi-scenario approach, Agric. For. Meteorol., 369, 110566, https://doi.org/10.1016/j.agrformet.2025.110566, 2025.

Goodrick, S. L.: Modification of the Fosberg fire weather index to include drought, Int. J. Wildl. Fire, 11, 205–211, https://doi.org/10.1071/WF02005, 2002.

He, Z., Fan, G., Li, Z., Li, S., Gao, L., Li, X., and Zeng, Z.-C.: Deep learning modeling of human activity affected wildfire risk by incorporating structural features: A case study in eastern China, Ecol. Indic., 160, 111946, https://doi.org/10.1016/j.ecolind.2024.111946, 2024.

Hirschberger: Forests Ablaze Cause and Effects of Global Forest Fires. WWF Deutschland. Berlin, DM, Germany. 107, https://www.wwf.de/fileadmin/fm-wwf/Publikationen-PDF/WWF-Study-Forests-Ablaze.pdf, 2016.

Hood, S. M., Varner, J. M., Jain, T. B., and Kane, J. M.: A framework for quantifying forest wildfire hazard and fuel treatment effectiveness from stands to landscapes, Fire Ecol., 18, 33, https://doi.org/10.1186/s42408-022-00157-0, 2022.

Huffman, G. J., Bolvin, R., Joyce, E. J., Tan, N. J., D, B., K, H., Kelley, P., Nguyen, S., Sorooshian, D. C., Watters, B. J., West, P., and Xie: Algorithm theoretical basis document (ATBD) NASAglobal precipitation measurement (GPM) integrated multi-satel-lite retrievals for GPM (IMERG) Version 07, Pps, 52, 2023.

IGP: Indicadores de la vegetación andina amazónica para la prevención de incendios forestales (2024-004). Instituto Geofísico del Perú. https://repositorio.igp.gob.pe/items/cf0cb87c-657c-4ee1-b420-8399399cc533, 2024

INM: Risco de Incêndio. Instituto Nacional de Meteorología, https://portal.inmet.gov.br/, 2026.

INPE: Incrementos de desmatamento - Amazônia Legal – estados (Instituto Nacional de Pesquisas Espaciais), https://terrabrasilis.dpi.inpe.br/app/dashboard/de, https://doi.org/https://terrabrasilis.dpi.inpe.br/app/dashboard/deforestation/biomes/legal_amazon/increments, 2021.

Ismail, F. N., Woodford, B. J., Licorish, S. A., and Miller, A. D.: An assessment of existing wildfire danger indices in comparison to one-class machine learning models, Nat. Hazards J. Int. Soc. Prev. Mitig. Nat. Hazards, 120, 14837–14868, https://doi.org/10.1007/s11069-024-06738-3, 2024.

Jimenez, J. C., Marengo, J. A., Alves, L. M., Sulca, J. C., Takahashi, K., Ferrett, S., and Collins, M.: The role of ENSO flavours and TNA on recent droughts over Amazon forests and the Northeast Brazil region, Int. J. Climatol., 41, 3761–3780,

https://doi.org/10.5194/egusphere-2026-1902
Preprint. Discussion started: 14 April 2026

https://doi.org/10.1002/joc.6453, 2021.

Keeley, J. E. and Syphard, A. D.: Large California wildfires: 2020 fires in historical context, Fire Ecol., 17, 22, https://doi.org/10.1186/s42408-021-00110-7, 2021.

Laneve, G., Pampanoni, V., and Uddien Shaik, R.: The Daily Fire Hazard Index: A Fire Danger Rating Method for Mediterranean Areas, Remote Sens., 12, https://doi.org/10.3390/rs12152356, 2020.

Li, X., Wu, T., Xia, K., Tang, H., Wang, X., Wang, S., Lyne, V., and Zu, Y.: Forest loss intensifies meteorological drought in more than half of Earth's climate zones, Sci. Adv., 12, eadv7998, https://doi.org/10.1126/sciadv.adv7998, 2026.

Marcuzzi, E., González, M., and Dentoni, M.: Forecasting the Danger of the Forest Fire Season in North-West Patagonia, Argentina, 257–271, https://doi.org/10.1007/978-3-031-04532-5_13, 2022.

Marengo, J. A. and Espinoza, J. C.: Extreme seasonal droughts and floods in Amazonia: causes, trends and impacts, Int. J. Climatol., 36, 1033–1050, https://doi.org/10.1002/joc.4420, 2016.

Marengo, J. A., Nobre, C. A., Tomasella, J., Oyama, M. D., de Oliveira, G. S., de Oliveira, R., Camargo, H., Alves, L. M., and Brown, I. F.: The drought of Amazonia in 2005, J. Clim., 21, 495–516, https://doi.org/10.1175/2007JCLI1600.1, 2008.

McArthur, A. G.: Fire behaviour in eucalypt forests. Leaflet (Australia. Forestry and Timber Bureau); no. 107., https://catalogue.nla.gov.au/catalog/2275488, 1967a.

McArthur, A. G.: Fire behaviour in eucalypt forests, 1967b.

Mestre, A. and Manta, M. I.: A fire weather index as a basis for an early warning system in Spain, Int. J. Wildl. Fire, 23, 510–519, https://doi.org/10.1071/WF13003, 2014.

MIDAGRI: Superficie Agrícola Peruana.Ministerio de Desarrollo Agrario y Riego, https://siea.midagri.gob.pe/portal/informativos/superficie-agricola-peruana, 2024.

MIDAGRI: Encuesta Nacional de Intenciones de Siembra. Ministerio de Desarrollo Agrario y Riego, https://siea.midagri.gob.pe/portal/informativos/enis, 2025a.

MIDAGRI: Encuesta Nacional de Intenciones de Siembra, 2025b.

MINAM: Memoria Descriptiva del Mapa Nacional de Ecosistemas del Perú. Ministerio del Ambiente, https://sinia.minam.gob.pe/normas/aprueban-mapa-nacional-ecosistemas-memoria-descriptiva-las-definiciones, 2019.

MINAM: Registro histórico de incendios sobre la cobertura vegetal a nivel nacional. Mapa de Condiciones favorables para la ocurrencia de incendios sobre la cobertura vegetal. Dirección General de Ordenamiento Territorial Ambiental (DGOTA). Ministerio del Ambient, https://geoservidor.minam.gob.pe/monitoreo-y-evaluacion/descarga-de-informacion/, 2025.

Mosquera-Guerra, F., Moreno-Niño, N., Garcia-Suabita, W., and Armenteras-Pascual, D.: Impact of wildfires on the suitability habitat of the lowland tapir in a native savanna landscape of northern South America, Discov. Conserv., 1, 15, https://doi.org/10.1007/s44353-024-00013-z, 2024.

Myers, N., Mittermeier, R. A., Mittermeier, C. G., da Fonseca, G. A. B., and Kent, J.: Biodiversity hotspots for conservation priorities, Nature, 403, 853–858, https://doi.org/10.1038/35002501, 2000.

Nesterov, V. .: Combustibility of the forest and methods for its determination., 1949.

Nunes, J. R. S., Soares, R. V., and Batista, A. C.: FMA+ - UM NOVO ÍNDICE DE PERIGO DE INCÊNDIOS FLORESTAIS PARA

O ESTADO DO PARANÁ, BRASIL, FLORESTA, 36, https://doi.org/10.5380/rf.v36i1.5509, 2006.

Pazmiño, D.: Peligro de incendios forestales asociado a factores climáticos en Ecuador, FIGEMPA Investig. y Desarro., 1, 10–18, https://doi.org/10.29166/revfig.v1i1.1800, 2019.

PCM: Declaran Estado de Emergencia por incendios forestales en varios distritos de los departamentos de Lambayeque y Cajamarca. DS 085-2016. Presidencia de Consejo de Ministros. Gobierno del Perú., https://sinia.minam.gob.pe/normas/declaran-estado-emergencia-incendios-forestales-varios-distritos, 2016.

PCM: Declaran Estado de Emergencia por incendios forestales en varios distritos de los departamentos de Lambayeque y Cajamarca. N° 097-2024-PCM, https://busquedas.elperuano.pe/dispositivo/NL/2326734-1, 2024a.

PCM: Decreto Supremo que declara el Estado de Emergencia en el departamento de Loreto, por peligro inminente ante déficit hídrico., 2024b.

Pivello, V. R., Vieira, I., Christianini, A. V, Ribeiro, D. B., da Silva Menezes, L., Berlinck, C. N., Melo, F. P. L., Marengo, J. A., Tornquist, C. G., Tomas, W. M., and Overbeck, G. E.: Understanding Brazil's catastrophic fires: Causes, consequences and policy needed to prevent future tragedies, Perspect. Ecol. Conserv., 19, 233–255, https://doi.org/10.1016/j.pecon.2021.06.005, 2021.

Potter, E. R., Fyffe, C. L., Orr, A., Quincey, D. J., Ross, A. N., Rangecroft, S., Medina, K., Burns, H., Llacza, A., Jacome, G., Hellström, R. Å., Castro, J., Cochachin, A., Montoya, N., Loarte, E., and Pellicciotti, F.: A future of extreme precipitation and droughts in the Peruvian Andes, npj Clim. Atmos. Sci., 6, 96, https://doi.org/10.1038/s41612-023-00409-z, 2023.

Pulgar Vidal, J.: Las ocho regiones naturales del Perú, Terra Bras., 3, https://doi.org/10.4000/terrabrasilis.1027, 2014.

Qadir, A., Talukdar, N. R., Uddin, M. M., Ahmad, F., and Goparaju, L.: Predicting forest fire using multispectral satellite measurements in Nepal, Remote Sens. Appl. Soc. Environ., 23, 100539, https://doi.org/10.1016/j.rsase.2021.100539, 2021.

dos Reis, M., Graça, P. M. L. de A., Yanai, A. M., Ramos, C. J. P., and Fearnside, P. M.: Forest fires and deforestation in the central Amazon: Effects of landscape and climate on spatial and temporal dynamics, J. Environ. Manage., 288, 112310, https://doi.org/10.1016/j.jenvman.2021.112310, 2021.

Roman, M., Zubieta, R., Ccanchi, Y., Martínez, A., Paucar, Y., Alvarez, S., Loayza, J., and Ayala, F.: Seasonal Effects of Wildfires on the Physical and Chemical Properties of Soil in Andean Grassland Ecosystems in Cusco, Peru: Pending Challenges, Fire, 7, https://doi.org/10.3390/fire7070259, 2024.

Rothermel, R.: A matematical model for fire spreadprediction. In Wildland fuels, USDA For. Serv. Ogden , Utah, EE.UU. Reseach Pap. INT-115., 1972.

Rouse J.~W., J., Haas, R. ~H., Schell, J. ~A., and Deering, D. ~W.: Monitoring Vegetation Systems in the Great Plains with Erts, in: NASA Special Publication, vol. 351, 309, 1974.

Saaty, T. L.: A scaling method for priorities in hierarchical structures, J. Math. Psychol., 15, 234–281, https://doi.org/10.1016/0022-2496(77)90033-5, 1977.

Saavedra, M. and Zubieta, R.: Monitoreo de días secos basado en datos de satélite (IMERG-L) de alta resolución espacio-temporal, https://repositorio.igp.gob.pe/server/api/core/bitstreams/beecced9-b907-42d5-be8a-9a6d5d9bebad/content, 2024.

Schmidt, I. B. and Eloy, L.: Fire regime in the Brazilian Savanna: Recent changes, policy and management, Flora, 268, 151613, https://doi.org/10.1016/j.flora.2020.151613, 2020.

Sharples, J. J., McRae, R. H. D., Weber, R. O., and Gill, A. M.: A simple index for assessing fuel moisture content, Environ. Model.

https://doi.org/10.5194/egusphere-2026-1902
Preprint. Discussion started: 14 April 2026

Softw., 24, 637–646, https://doi.org/10.1016/j.envsoft.2008.10.012, 2009.

Silva, I. D. B., Valle, M. E., Barros, L. C., and Meyer, J. F. C. A.: A wildfire warning system applied to the state of Acre in the Brazilian Amazon, Appl. Soft Comput., 89, 106075, https://doi.org/10.1016/j.asoc.2020.106075, 2020.

Silva, P. S., Libonati, R., Gonçalves, L. G., and DaCamara, C. C.: The climatic patterns that control regional fire activity in the Brazilian savanna, Agric. For. Meteorol., 374, 110792, https://doi.org/10.1016/j.agrformet.2025.110792, 2025.

Silva, S. S. da, Oliveira, I., Morello, T. F., Anderson, L. O., Karlokoski, A., Brando, P. M., Melo, A. W. F. de, Costa, J. G. da, Souza, F. S. C. de, Silva, I. S. da, Nascimento, E. de S., Pereira, M. P., Almeida, M. R. N. de, Alencar, A., Aragão, L. E. O. e C. de, Brown, I. F., Graça, P. M. L. de A., and Fearnside, P. M.: Burning in southwestern Brazilian Amazonia, 2016–2019, J. Environ. Manage., 286, 112189, https://doi.org/10.1016/j.jenvman.2021.112189, 2021.

Soto, M. C., Julio-Alvear, G., and Salinas, R. G.: Current Wildfire Risk Status and Forecast in Chile, in: Wildfire Hazards, Risks and Disasters, edited by: Shroder, J. F. and Paton, D., Elsevier, Oxford, 59–75, https://doi.org/10.1016/B978-0-12-410434-1.00004-X, 2015.

Srock, A. F., Charney, J. J., Potter, B. E., and Goodrick, S. L.: The Hot-Dry-Windy Index: A New Fire Weather Index, Atmosphere (Basel)., 9, https://doi.org/10.3390/atmos9070279, 2018.

Sulca, J., Vuille, M., Timm, O. E., Dong, B., and Zubieta, R.: Empirical–Statistical Downscaling of Austral Summer Precipitation over South America, with a Focus on the Central Peruvian Andes and the Equatorial Amazon Basin, J. Appl. Meteorol. Climatol., 60, 65–85, https://doi.org/10.1175/JAMC-D-20-0066.1, 2021.

Taboada-Hermoza, R. and Martínez, A. G.: "No One Is Safe": Agricultural Burnings, Wildfires and Risk Perception in Two Agropastoral Communities in the Puna of Cusco, Peru, Fire, 8, https://doi.org/10.3390/fire8020060, 2025.

Talukdar, N. R., Ahmad, F., Goparaju, L., Choudhury, P., Arya, R., Qayum, A., and Rizvi, J.: Forest fire estimation and risk prediction using multispectral satellite images: Case study, Nat. Hazards Res., 4, 304–319, https://doi.org/10.1016/j.nhres.2024.01.007, 2024.

Toledo, N., Moulatlet, G., Gaona, G., Valencia, B., Hirata, R., and Conicelli, B.: Dynamics of meteorological and hydrological drought: The impact of groundwater and El Niño events on forest fires in the Amazon, Sci. Total Environ., 954, 176612, https://doi.org/10.1016/j.scitotenv.2024.176612, 2024.

UP: Evidencia para una Nueva Gestión Pública. Universidad del Pacífico., https://www.up.edu.pe/egp/programas-especializacion_copy(1)/SiteAssets/Lists/Observatorio/AllItems/Informe de Evidencia sector Agropecuario - EGP.pdf, 2022.

Vermote, E. F., El Saleous, N. Z., and Justice, C. O.: Atmospheric correction of MODIS data in the visible to middle infrared: first results, Remote Sens. Environ., 83, 97–111, https://doi.org/10.1016/S0034-4257(02)00089-5, 2002.

Van Wagner, C. E.: Structure of the Canadian forest fire weather index, http://cfs.nrcan.gc.ca/pubwarehouse/pdfs/19927.pdf, 1974.

Van Wagner, C. E.: Development and structure of the Canadian Forest Fire Weather Index System., http://cfs.nrcan.gc.ca/pubwarehouse/pdfs/19927.pdf, 1987.

Waidelich, S., Zimmerman, V., Laneri, K., and ...: Fire weather index assessment and visualization, … 14 Al 18 Oct. …, 140–149, 2019.

Woodman, R. and Takahashi, K.: ¿ Por que no llueve en la costa?. Programa Presupuestal por Resultados No 068, https://repositorio.igp.gob.pe/server/api/core/bitstreams/e73dd2d6-44ae-4f26-9ed9-4ffbb5d892c4/content, 2014.

Xofis, P., Tsiourlis, G., and Konstantinidis, P.: A Fire Danger Index for the early detection of areas vulnerable to wildfires in the Eastern

https://doi.org/10.5194/egusphere-2026-1902
Preprint. Discussion started: 14 April 2026

Mediterranean region, Euro-Mediterranean J. Environ. Integr., 5, 32, https://doi.org/10.1007/s41207-020-00173-z, 2020.

Xu, Z., Li, J., Cheng, S., Rui, X., Zhao, Y., He, H., Guan, H., Sharma, A., Erxleben, M., Chang, R., and Xu, L. L.: Deep learning for wildfire risk prediction: Integrating remote sensing and environmental data, ISPRS J. Photogramm. Remote Sens., 227, 632–677, https://doi.org/10.1016/j.isprsjprs.2025.06.002, 2025.

Yebra, M., Dennison, P. E., Chuvieco, E., Riaño, D., Zylstra, P., Hunt, E. R., Danson, F. M., Qi, Y., and Jurdao, S.: A global review of remote sensing of live fuel moisture content for fire danger assessment: Moving towards operational products, Remote Sens. Environ., 136, 455–468, https://doi.org/10.1016/j.rse.2013.05.029, 2013.

Ziccardi, L. G., Thiersch, C. R., Yanai, A. M., Fearnside, P. M., and Ferreira-Filho, P. J.: Forest fire risk indices and zoning of hazardous areas in Sorocaba, São Paulo state, Brazil, J. For. Res., 31, 581–590, https://doi.org/10.1007/s11676-019-00889-x, 2020.

Zubieta, R., Prudencio, F., Alarco, G., and Reupo, J.: Ocurrencia de incendios forestales en el Perú durante eventos El Niño. Boletín Técnico El Niño. Instituto Geofísico del Perú, https://repositorio.igp.gob.pe/items/7450d933-5794-47ba-8bbc-d1099581f664, 2019.

Zubieta, R., Molina-Carpio, J., Laqui, W., Sulca, J., and Ilbay, M.: Comparative Analysis of Climate Change Impacts on Meteorological, Hydrological, and Agricultural Droughts in the Lake Titicaca Basin, Water, 13, https://doi.org/10.3390/w13020175, 2021a.

Zubieta, R., Prudencio, F., Ccanchi, Y., Saavedra, M., Sulca, J., Reupo, J., and Alarco, G.: Potential conditions for fire occurrence in vegetation in the Peruvian Andes, Int. J. Wildl. Fire, 30, 836–849, https://doi.org/10.1071/WF21029, 2021b.

Zubieta, R., Ccanchi, Y., and Liza, R.: Performance of heat spots obtained from satellite datasets to represent burned areas in Andean ecosystems of Cusco, Peru, Remote Sens. Appl. Soc. Environ., 32, 101020, https://doi.org/10.1016/j.rsase.2023.101020, 2023a.

Zubieta, R., Ccanchi, Y., Martínez, A., Saavedra, M., Norabuena, E., Alvarez, S., and Ilbay, M.: The role of drought conditions on the recent increase in wildfire occurrence in the high Andean regions of Peru, Int. J. Wildl. Fire, 32, 531–544, https://doi.org/10.1071/WF21129, 2023b.